CHEMICAL DEGRADATION ASSESSMENT OF CEMENTITIOUS MATERIALS FOR THE HLW TANK CLOSURE PROJECT (U)

September 14, 2007

Washington Savannah River Company
Savannah River National Laboratory
Aiken, SC 29808

Prepared for the U.S. Department of Energy
Under Contract No. DE-AC09-96SR18500

SRNL
SAVANNAH RIVER NATIONAL LABORATORY

Printed in the United States of America

Prepared For
U.S. Department of Energy

WSRC-STI-2007-00607, Rev 0

Key Words: Tank PA
Concrete Degradation
Concrete Service Life

CHEMICAL DEGRADATION ASSESSMENT OF CEMENTITIOUS MATERIALS FOR THE HLW TANK CLOSURE PROJECT (U)

C. A. Langton

Savannah River National Laboratory
Washington Savannah River Company
Aiken, SC 29809

September 15, 2007

Washington Savannah River Company
Savannah River National Laboratory
Aiken, SC 29808

Prepared for the U.S. Department of Energy
Under Contract No. DE-AC09-96SR18500

SRNL
SAVANNAH RIVER NATIONAL LABORATORY

REVIEWS AND APPROVALS

Authors:

Christine A. Langton 10-23-07
C. A. Langton, SRNL / Process Science & Engineering Date

Reviewers:

10/23/07
S. E. Aleman, SRNL / Eng, Modeling & Simulation (Calculation Review) Date

John R Harbour 10/25/07
J. R. Harbour, SRNL / Process Science & Engineering Date

SRNL Management Approvals:

10/29/07
D. K. Peeler, SRNL / Process Science & Engineering Date

David A. Crowley 10/29/07
D. A. Crowley, Manager, SRNL / Stabilization Science Research Date

David A. Crowley for 10/29/07
R. E. Edwards, Manager, SRNL / Process Science & Engineering Date

Customer Approvals:

10/29/07
R. Deshpande, Site Regulatory Interface & Planning Date

Kent H. Rosenberg for 10/29/07
T. C. Robinson, Jr., Site Regulatory Interface & Planning Date

TABLE OF CONTENTS

LIST OF TABLES

LIST OF FIGURES

List of Acronyms

AAR	Alkali Aggregate Reaction
ACI	American Concrete Institute
ASTM	American Society for Testing and Materials
AFm	(Al2O3-Fe2O3-mono) phases[1]
AFt	(Al2O3-Fe2O3-tri) phases[2]
C-S-H	Calcium silicate hydrate
DEF	Delayed Ettringite Formation
ERDMS	Environmental Restoration Data Management System
FTF	F-Area Tank Farm
g	gram
HLW	High Level Waste
INEEL	Idaho National Engineering and Environmental Laboratory
K_{isat}	Initial Saturated Hydraulic Conductivity
LLW	Low Level Waste
mL	milliliter
NIST	National Institute of Standards and Testing
Pa	Pascal
PA	Performance Assessment
PS&E	Process Science and Engineering
psi	pounds per square inch
RH	Relative Humidity
SRIP	Site Regulatory Interface and Planning
SRNL	Savannah River National Laboratory
SRS	Savannah River Site
TS	Total Solids
WSRC	Washington Savannah River Company
Wt	Weight
Wt%	Weight percent

[1] General formula is $[Ca_2(Al,Fe)(OH)_6]\cdot X\cdot xH_2O$ where X denotes one formula unit of a singly charged anion or ½ of a doubly charged anion.

[2] General formula is $[Ca_3(Al,Fe)(OH)_6\cdot 12H_2O]_2\cdot 3X\cdot xH_2O$ where X is < or = 2 and represents one formula unit of a doubly charged anion or 2 formula units of a singly charged anion.

1.0 SUMMARY

The objective of this task was to provide estimates of the effects and extent of chemical degradation of the cementitious barriers used or planned to be used in the Savannah River Site (SRS) F-Tank Farm closure concept. This information is intended to be used to estimate the hydraulic conductivity of the barriers as a function of time which is required as input for the SRS F-Tank Farm (FTF) Closure Performance Assessment (PA). The approach taken included:

- Reviewing the F-Tank Farm Closure concept and developing a simplified model for evaluating degradation of the cementitious barriers.
- Reviewing causes for concrete structure failures.
- Reviewing properties of the cementitious materials that control transport of corrosive agents in the concrete.
- Identifying potential chemical degradation mechanisms.
    - Chemical degradation processes included, sulfate attack, alkali aggregate attack, acid leaching (decalcification), carbonation, and rebar corrosion.
    - Chemical degradation processes not evaluated were wet-dry cycling and freeze-thaw cycling because these processes are not included in the scenarios considered in the PA.
- Identifying rate controlling factors and data required to calculate degradation rates.
- Calculating depth of degradation (thickness of the degraded zone) assuming that spatial transport of chemical species coincides with degradation.
    - Concrete degradation rate equations used in the Idaho National Engineering and Environmental Laboratory (INEEL) PA Appendix E, 1990, were used for this analysis per request by the customer, Site Regulatory Interface and Planning [Robinson, 2007]. The bases for these equations and application to modeling service life of concrete barriers for low-level radioactive waste disposal are discussed in detail elsewhere [Walton, et al., 1990].
- Correlating the depth of penetration to microstructure and cracking,both of which affect hydraulic permeability.

Based on this review, the current SRS F-Tank Farm disposal environment was found to be very benign with respect to chemical degradation of the reinforced concrete vaults and the tank fill grout material. Consequently, the degradation due to chemical processes will progress at a very slow rate. Simple empirical relationships or single phase diffusion equations were used to calculate distance of transport of the potentially corrosive species. This approach can over or under estimate the rate of loss of intact material because it does not take into account non deleterious binding reactions, activation energies, threshold values for initiation of corrosion, etc. On the other hand it does not take into account coupled effects.

The penetration depth of the chemical species responsible for the degradation was assumed to be equivalent to the depth of degradation. The consequences of the degradation depended on the material porosity and whether or not the material contained steel reinforcing because steel rebar introduces an additional degradation process, i.e., concrete cracking due to formation of expansive metal corrosion products.

Porosity data for two representative materials were used in calculations to predict the depth of penetration of the various forms of chemical attack. These materials were a surrogate base mat concrete (29 year 3000 psi concrete from P-Area, SRS) which represented the vault concrete and a tank fill reducing grout which represented all of the fill grout in the tanks and the annulus spaces.

The most extensive attack was from carbonation. Carbonation was found to result in the greatest penetration as a function of time. For material with the porosity of the surrogate base mat concrete, 16.8 volume percent, the depth of penetration from carbonation was estimated to be 21 cm after 1000 years. The estimated depth of penetration for the representative fill grout from carbonation reactions was 36 cm after 1000 years. (The source of carbonate was assumed to be the atmosphere.)

The impact of carbonation on the permeability of the cementitious barriers in the FTF closure concept depends on whether the barrier contains steel. Carbonation in itself may actually reduce permeability by plugging pores with calcium carbonate. However, it will affect the permeability of reinforced concrete because the concrete will crack due to formation of expansive iron hydroxide phases which form when steel corrodes. Steel passivation is lost when the pH of the pore solution is in equilibrium with calcium carbonate (pH~8.4) rather than calcium hydroxide (pH~12.5).

The consequences of carbonation with respect to the permeability of the cementitious barriers in the FTF depend on the assumptions made to link depth of penetration with formation of expansive iron hydroxide phase from associated rebar corrosion and the assumptions linking corrosion with concrete cracking.

For the reinforced vault concrete, the assumption that cracking occurs simultaneously with carbonation is unrealistic. Cracking will lag the carbonation by a considerable time especially in the absence of other corrodents such as chloride ion. When cracking from expansion does occur, the permeability will increase. Permeability values for degraded FTF vault concrete have not been measured but are assumed to be the same as the infill soil above the tank. This is a reasonable assumption (100 times increase) given the lack of data.

Because the annulus fill grout and fill grout in the tanks without cooling coils do not contain rebar or steel, the overall effect of carbonation should be minimal regardless of the depth of penetration. The permeability of these materials is not expected to change significantly as the result of carbonation. This is the case even though the rate of carbonate penetration is faster due to the higher porosity of the fill grout (26.6 volume percent).

Carbonation of the tank fill grout will not commence until the tank is breached due to corrosion or development of a fast pathway. Based on calculated tank corrosion rates [Subramanian, 2007] a lengthy lag time is anticipated before carbonate actually contacts the grout and the carbonation front advances to the cooling coils. The corrosion rate is expected to be very slow in the absence of additional corrodents.

The impact of carbonation on cracking when it does occur is expected to be the same as described above. The permeability of the degraded concrete could increase as much as 100 times. However, the possibility exists that expansive reactions occurring in under the

somewhat constrained conditions of the buried tank could result in very little change in permeability. This can be further evaluated by requesting a mechanical analysis be performed by the appropriate personnel in the SRS design integration organization or by a qualified subcontractor.

A more sophisticated approach requires additional material characterization data and advanced multi ionic transport codes specially designed for concrete service life predictions. (These codes are limited in that they have been tested for performance over relatively short performance times of 20-50 years.)

1.1 References

INEEL PA Appendix E, 2003. "Degradation Analysis of the Grouted Tank/vault and Piping System at the Idaho Nuclear Technology and Engineering Center Tank Farm Facility and Preliminary Results for the Detailed Analysis of Releases from the Grouted Pipe and Encasement System, Revision 1,"p. E15, E20, INEEL, Idaho Falls, ID, 2003.

Subramanian, K.H., 2007. "Life Estimation of High Level Waste Tank Steel for F-tank Farm Closure Performance Assessment," WSRC-STI-2007-00061, Rev. 1. October 1-2007, Washington Savannah River Company, Aiken SC 29808.

Robinson, T.C. Jr., 2007. Personal communication with C.A. Langton, W.E. Stevens, M.H. Layton, and J.L. Newman 2007, Washington Savannah River Company, Aiken SC 29808.

Walton, J.C., L.E. Plansky and R.W. Smith, 1990. "Models for Estimation of Service Life of Concrete Barriers in Low-Level Radioactive Waste Disposal," NUREG/CR—5542, TI91 000576, EG&G Idaho, Inc., Idaho Falls, ID 83415.

2.0 INTRODUCTION

2.1 Objective and Approach

The objective of this task was to provide estimates of the effects and extent of chemical degradation of the cementitious barriers used or planned to be used in the SRS F-Tank Farm closure concept. These estimates are intended to be used in the SRS F-Tank Farm Closure Performance Assessment (PA). The approach taken included:

- Reviewing the F-Tank Farm Closure concept and developing a simplified model for evaluating degradation of the cementitious barriers.
- Reviewing causes for concrete structure failures.
- Reviewing properties of the cementitious materials that control transport of corrosive agents in the concrete.
- Identifying potential chemical degradation mechanisms.
    - Chemical degradation processes included: sulfate attack, alkali aggregate attack, acid leaching (decalcification), carbonation, and rebar corrosion.
    - Chemical degradation processes not evaluated were wet-dry cycling and freeze-thaw cycling because these processes are not included in the scenarios considered in the PA.
- Identifying rate controlling factors and data required to calculate rates.
- Calculating depth of degradation (thickness of the degraded zone) assuming that spatial transport of chemical species coincides with degradation.
- Estimating the impact of chemical degradation processes on the permeability of the tank vault concrete and tank fill grouts.

Simple empirical relationships or single phase diffusion equations were used to calculate distance of transport of the potentially corrosive species. These equations and approach were developed by Walton, et al, 1990, and were used in the INEEL PA Appendix E, 2003.

Advanced service life prediction models for concrete structures, such as Stadium®, SIMCO Technologies, Inc., were not used because these models require concrete-specific properties, such as, moisture, ionic, and gas diffusion coefficients, pore solution chemistry, porosity, pore size distribution, degree of saturation, cement chemistry and mineralogy, and thickness of rebar cover. They also required environment-specific characterization data.

2.2 Background

2.2.1 SRS HLW Tanks

Conceptual drawings of the four types of F-Area high-level waste (HLW) tanks are provided in Figure 2-1. The tank system consists of:

- Cylindrical carbon steel waste tank with steel cooling coils distributed throughout the entire tank volume.
    - Type IV tanks do not contain cooling coils.
- An annulus space separating the steel waste tank from the secondary containment.

  - Type IV tanks do not have an annulus space between the steel tank and concrete vault.
- Secondary containment consisting of:
  - A partial (Type I) or full height (Type III and Type IIIA) carbon steel liner (open top).
  - Type IV tanks do not have secondary containment.
- An outer cylindrical concrete vault (base mat, wall, and roof).

A list of the cementitious materials used and planned to be used as fill materials in the F-Tank Farm closure is provided in Table 2-1.

2.2.2 SRS HLW Tank Closure Concept

The F-Tank Farm (FTF) conceptual closure model is illustrated in Figure 2-2. The closure plan involves:

- Removing as much waste as practical from the tank
- Completely filling the emptied tank with cementitious material to physically and chemically stabilize any remaining radionuclides. The objective of physical and chemical stabilization are to:
  - Eliminate voids and thereby prevent subsidence and accumulation of infiltration water, "bath tub effect"
  - Create a chemical environment that retards the mobility of radionuclides and thereby reduces the impact on the environment.
- Completely filling the annulus space between the steel tank and concrete vault (Types I, III, and IIIA tanks) and the riser accesses in the top of the tanks to eliminate voids and pathways for water.
- Filling cooling coils in the Type I, III, and IIIA tanks to minimize fast pathways for infiltration water.

2.2.3 Vault Concrete and Cementitious Fill Properties for PA Modeling

For the PA modeling all of the concrete materials used in construction of the tanks in the F-Tank Farm consolidated in to two generic materials, surrogate reinforced concrete and representative reducing grout. Since the actual tank vault concrete is not readily accessible, a surrogate material was used to obtain property data. The surrogate material was collected from a slab constructed in 1978 in P-Area. This material is a 3000 psi reinforced concrete containing Type I Portland cement and local aggregates [DuPont, 1978]. The slab was constructed on grade such that the bottom was exposed to unsaturated soil and the top surface was exposed to ambient outdoor conditions. Hydraulic properties and sorption properties of this surrogate material were measured and are reported elsewhere [Dixon, 2007 and Kaplan, 2006 and 2007 (a), (b), (c) respectively].

In the PA modeling, all of the grout fill material was represented by a reducing grout, Mix No. OPDEXE-X-P-0-BS, described in WSRC Specification C-SPP-F-00047, Revision 2, Section 03311, paragraph 2. The hydraulic properties of these materials are provided in Table 2-2.

Typical Type I Waste Tank Modeling Dimensions

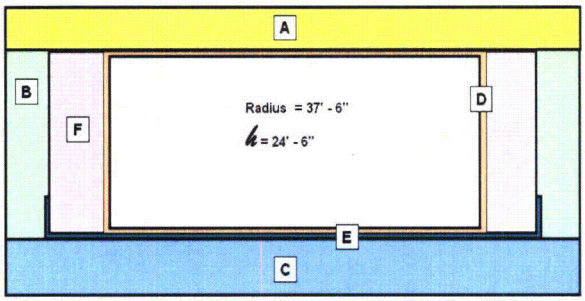

[NOT TO SCALE]

LABEL	THICKNESS	MATERIAL
A Concrete Roof	22"	Concrete (Dupont Spec 3019, Sec. B)
B Concrete Wall	22"	Concrete (Dupont Spec 3019, Sec. B)
C Concrete Basemat	30"	Concrete (Dupont Spec 3019, Sec. B)
D Primary Liner	0.5"	Carbon Steel (ASTM A-285-50T)
E Secondary Liner	5' high and 0.5" thick	Carbon Steel (ASTM A-285-50T)
F Grouted Annulus	30"	Tank Fill Grout

Typical Type III Waste Tank Modeling Dimensions

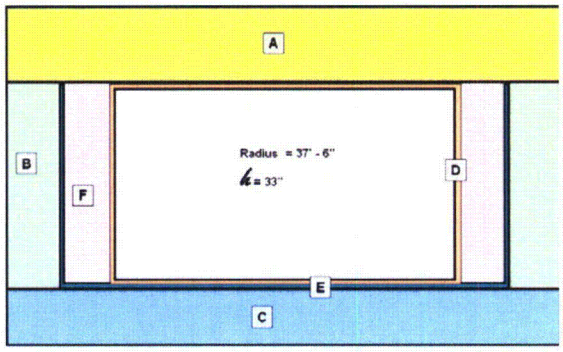

[NOT TO SCALE]

LABEL	THICKNESS	MATERIAL
A Concrete Roof	48"	Class C Concrete
B Concrete Wall	30"	Class C Concrete
C Concrete Basemat	42"	Class C Concrete
D Primary Liner	0.5"	Carbon Steel (ASTM A-516)
E Secondary Liner	3/8"	Carbon Steel (ASTM A-516)
F Grouted Annulus	30"	Tank Fill Grout

Typical Type IIIA Waste Tank Modeling Dimensions

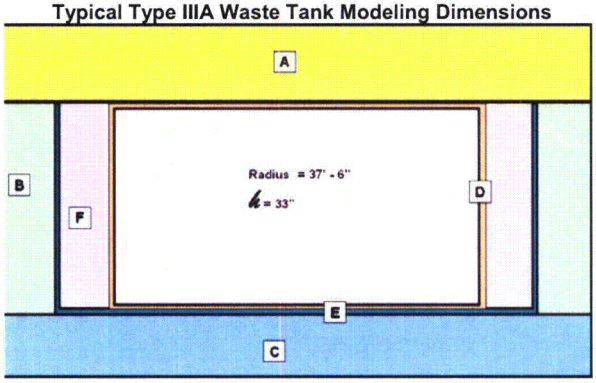

[NOT TO SCALE]

LABEL	THICKNESS	MATERIAL
A Concrete Roof	48"	Class C Concrete
B Concrete Wall	30"	Class C Concrete
C Concrete Basemat	41"	Class C Concrete
D Primary Liner	0.5"	Carbon Steel (Tanks 25 - 28: ASTM A-516) (Tanks 44 - 47: ASTM A-537)
E Secondary Liner	3/8"	Carbon Steel (Tanks 25 - 28: ASTM A-516) (Tanks 44 - 47: ASTM A-537)
F Grouted Annulus	30"	Tank Fill Grout

Typical Tank IV Modeling Dimensions

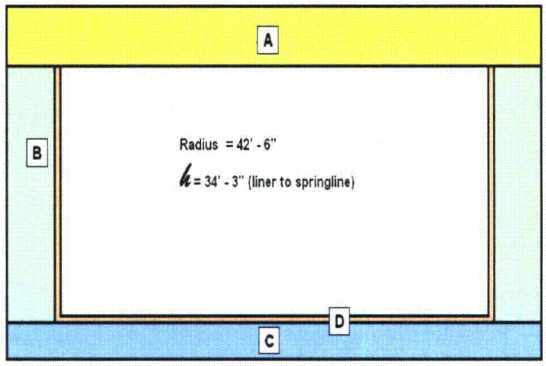

[NOT TO SCALE]

LABEL	THICKNESS	MATERIAL
A Concrete Roof	7"	Class A Concrete
B Concrete Wall	7"	Type I Portland Cement
C Concrete Basemat	6.9025"	Class C Concrete
D Primary Liner	0.375"	Carbon Steel (ASTM A-285-50T)

Figure 2-1. Schematic drawings and dimensions of the tanks in the F-Area Tank Farm [K. Rosenberger and T. Robinson, 2007, R. Deshpande, 2007.].

Table 2-1. Summary of cementitious material used to construct and close the F-Area Tank Farm [K. Rosenberger and T. Robinson, 2007, R. Deshpandel, 2007].

APPLICATION	MATERIAL	REINFORCEMENT	THICKNESS	
VAULT			**(inches)**	**(m)**
Type I				
Roof	Concrete DuPont Spec. 3019 Section B	Yes	22	0.56
Wall		Yes	22	0.56
Floor/ Base Mat		Yes	30	0.76
Type III				
Roof	DuPont Spec Class C Concrete	Yes	48	1.22
Wall		Yes	30	0.76
Floor/ Base Mat		Yes	42	1.07
Type IIIA				
Roof	DuPont Spec Class C Concrete	Yes	48	1.22
Wall		Yes	30	0.76
Floor/ Base Mat		Yes	41	1.04
Type IV				
Roof	Class C Concrete	Yes	7	0.178
Wall	Type I Portland Cement	Yes	7	0.178
Floor/ Base Mat	Class C Concrete	Yes	6.9	0.175
FILL				
Type I,				
Tank	TBD	No	Cylinder 24.5 ft high, 75 ft diameter	Cylinder 7.47 m high, 22.86 m diameter
Annulus	TBD	No	Cylindrical shell 30 ft high, OD ~ 77.5ft ID ~ 75ft	Cylindrical shell 9.14 m high, OD ~ 23.62 m ID ~ 22.86 m
Cooling Coil	TBD	No	2 ID	0.05
Riser	TBD	No		
TypeIII, IIIA				
Tank	TBD	No	Cylinder 33 feet high, 75 ft diameter	Cylinder 7.47 m high, 22.86 m diameter
Annulus	TBD	No	Cylindrical shell 30 ft high, OD ~ 77.5ft ID ~ 75ft	Cylindrical shell 9.14 m high, OD ~ 23.62 m ID ~ 22.86 m
Cooling Coil	TBD	No	2 ID	0.051
Riser	TBD	No		
Type IV				
Tanks 17 and 20	Reducing Grout (contact with residual waste) Bulk Fill Strong Grouts (top layer, intruder barrier)	No	Cylinder 34.25 feet high, 85 ft diameter	25.91
Tanks 18 and 19	Reducing Grout (contact with waste and bulk fill) Strong Grout (top layer, intruder barrier)*	No	Cylinder 34.25 feet high, 85 ft diameter	25.91
Annulus	NA	No	0	0
Cooling Coil	NA	No	NA	NA
Riser	5000 psi Grout	No	NA	NA

* SRS Specification C-SPP-F-00047, Revision 2, 2003 identifies Reducing Grout. However, the specification may be revised prior to closing Tanks 18 and 19.

NA = Not Applicable

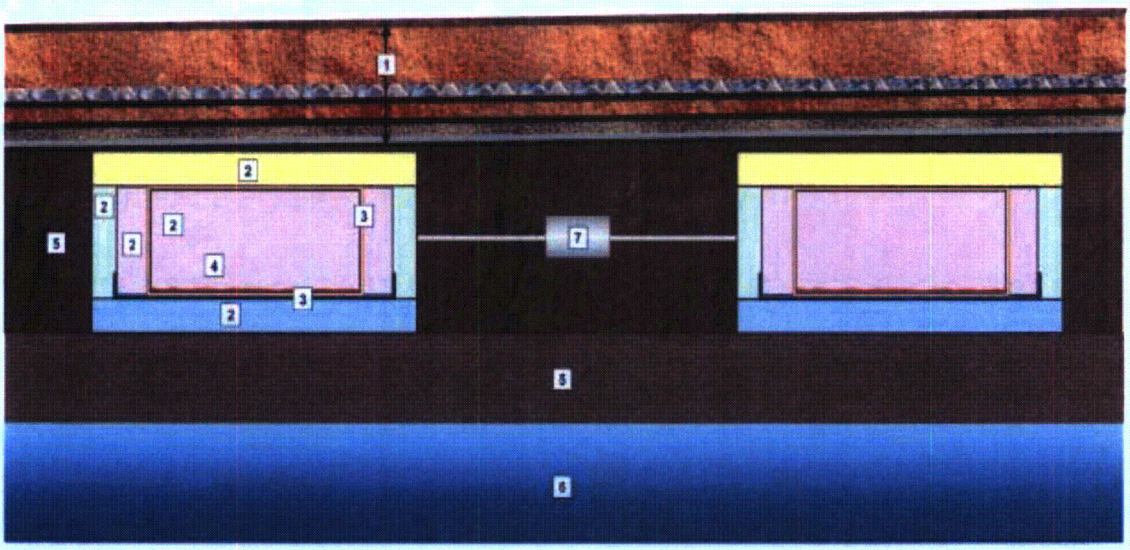

1 **Closure Cap** - Provides water flux to the top of tank from infiltrating rainwater.

2 **Vault Concrete and Tank Fill Grout** - Provides degradation description of the concrete and grout based materials in the tank system.

3 **Carbon Steel Tank Liner (Primary and Secondary)** - Provides degradation description of the carbon steel liners in the tank system.

4 **Contamination Leaching** - Provides waste contamination release rates of residual waste heel based on solubility and sorption rates per nuclide.

5 **Vadose Zone and Backfill** - Provides hydraulic related values for the unsaturated undisturbed soil beneath the tanks and the backfill soil surrounding the tanks.

6 **Hydrogeology** - Provides hydraulic related values for the saturated soil beneath the tanks.

7 **Ancillary Equipment** - Provides waste contamination release rates of residual waste associated with ancillary equipment.

Figure 2-2. F-Area Tank Farm conceptual closure model [K. Rosenberger and T. Robinson, 2007].

Table 2-2. Properties of the cementitious barriers used in the F-Area Tank Farm PA.

Cementitious Barrier	Ave. Permeability (cm/s)	Ave. Bulk Density (g/cm^3)	Ave. Water Exchangeable Porosity (fraction)
Tank Vault Concrete Surrogate 3000 psi reinforced concrete from [DuPont, 1978]	3.4E-08	2.06	0.168
Tank Fill Reducing Grout Mix No. OPDEXE-X-P-0-BS [WSRC, 2003]	3.6E-08	1.81	0.266

2.2.4 PA Environmental Scenarios and Cementitious Barrier Degradation Scenarios

Several environmental scenarios were assumed in the F-Area Tank Farm PA. Three scenarios are illustrated in Figure 2-3. These scenarios were selected to illustrate the range of conditions that are considered in the analysis. They include an intact tank unit (concrete vault, steel tank, and fill grout) in unsaturated soil, a closed tank that develops fast flow paths in unsaturated soil, and a closed tank in saturated soil assuming a rise in the water table.

The properties of degraded vault concrete and fill grout have not been measured. For the PA modeling, all of the cementitious barriers were assumed to degrade to material with the properties of soil used as infill above the tanks and are listed in Table 2-3 [M. Layton, 2007, Dixon and Phifer, 2007].

Table 2-3. Properties assumed for degraded cementitious barriers used in the F-Tank Farm PA [Layton, 2007, Dixon and Phifer, 2007].

Cementitious Barrier	**Ave. Permeability** (cm/s)	**Ave. Bulk Density** (g/cm3)	**Ave. Water Exchangeable Porosity** (fraction)
Degraded Cementitious Barrier (Vault Concrete and Fill grouts)	3.60E-06	1.81	26.6

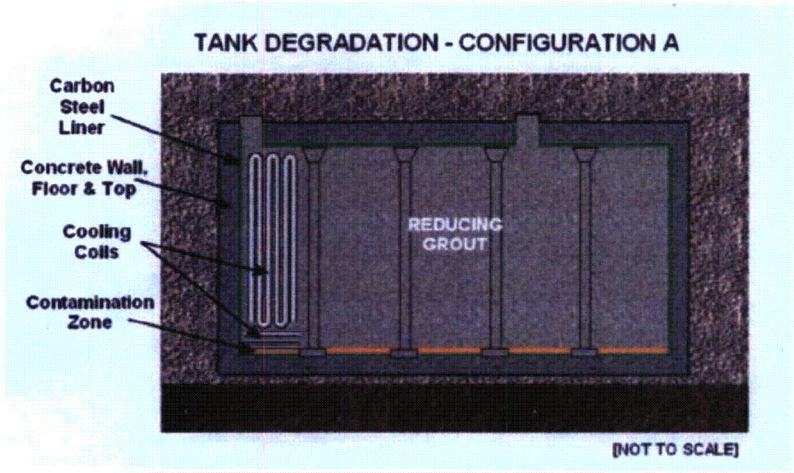

Unsaturated soil (50 -100 %) saturation transients in response to rainfall events

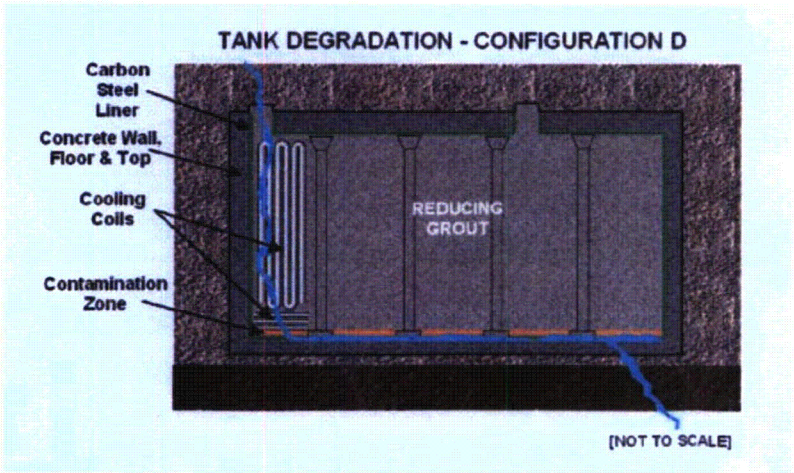

Fast Pathways from cracking

Unsaturated soil experiencing transient saturation in response to rainfall events

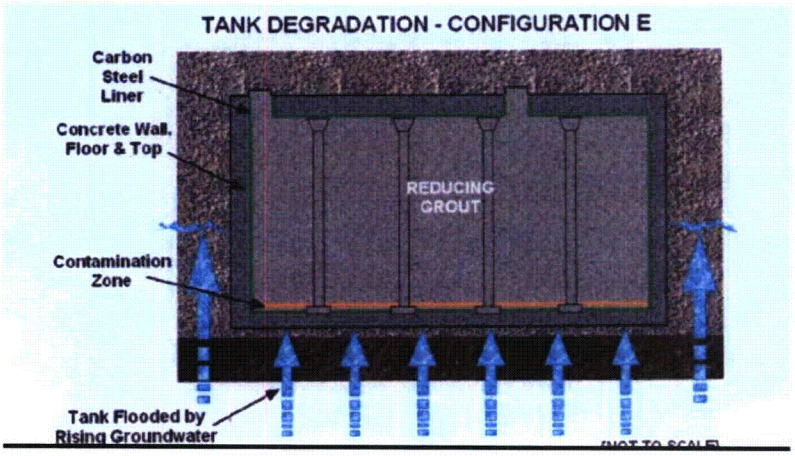

Saturated soil due to rise in water table

Figure 2-3. Examples for degradation scenarios for closed tanks [K. Rosenberger and T. Robinson, 2007].

2.3 References

Deshpandel, R., 2007. Personal communication October, 20007.

Dixon, K.L. and M.A. Phifer, 2007. "Hydraulic and Physical Properties of Tank Grouts for FTF Closure," WSRC-STI-2007-00369, Revision 0, October 2007, Washington Savannah River Company, Aiken SC 29808.

DuPont, 1978. Drawing W707379 Rev. 18., Project 151745, Building 904-86G-1, Savannah River Plant, Aiken SC.

INEEL PA Appendix E, 2003. "Degradation Analysis of the Grouted Tank/vault and Piping System at the Idaho Nuclear Technology and Engineering Center Tank Farm Facility and Preliminary Results for the Detailed Analysis of Releases from the Grouted Pipe and Encasement System, Revision 1,"p. E15, E20, INEEL, Idaho Falls, ID, 2003.

Kaplan, D. I., 2006. "Geochemical data Package for Performance Assessment Calculations Related to the Savannah River Site (U)," SRC-TR-2006-00004 Rev.0, February 28, 2006, Washington Savannah River Company, Aiken SC 29808.

Kaplan, D. I., 2007. "Distribution Coefficients for Various Elements of Concern to the Tank Waste Performance Assessment," SRNL-RPA-2007-00006, July 10, 2007, Washington Savannah River Company, Aiken SC 29808.

Kaplan, D. I., 2007. "Subject: K_d Values," E-mail to Rea Cauthen, July 16, 2007, Washington Savannah River Company, Aiken SC 29808.

Kaplan, D. I., 2007. "Concrete K_d Values Appropriate for the Tank Closure Performance Assessment," SRNL-RP-2007-01122, October 11, 2007, Washington Savannah River Company, Aiken SC 29808.

Layton, M. H., 2007. Personal Communication with G. Flach, SRNL, concerning material properties used in the 2007 Tank Closure PA Analysis. Reported values provided by G. P. Flach, October 23, 2007, Washington Savannah River Company, Aiken SC 29808.

Robinson, T., 2007, Personal communication, August, 20007, Washington Savannah River Company, Aiken SC 29808.

Rosenberger, K., 2007, Personal communication, August, 20007, Washington Savannah River Company, Aiken SC 29808.

WSRC, 2003. "Tank Farm: Tank 18F and Tank 19F, Furnishing and Delivery of Tank Closure Mixes (U)," SRS Specification C-SPP-F-00047, Revision 2, 2003, March 2, 2003 Washington Savannah River Company, Aiken SC 29808.

Walton, J.C., L.E. Plansky and R.W. Smith, 1990. "Models for Estimation of Service Life of Concrete Barriers in Low-Level Radioactive Waste Disposal," NUREG/CR—5542, TI91 000576, EG&G Idaho, Inc., Idaho Falls, ID 83415.

3.0 MICROSTRUCTURE OF HYDRATED CEMENT

3.1 Pore Structure and Water Classification

Characterization of the pore structures of cementitious materials is essential to evaluating saturated and unsaturated transport phenomena in these materials. Concrete and grout consist of aggregates and hardened cement paste which is a rigid gel with a high porosity and high internal surface area [Taylor, 1997].[3] Assuming that dense, nonporous aggregate is used in concrete, the porosity of concrete is a function of the water and relative proportion between the water and cement in the mix design.[4]

During hydration of the cement, mixing water is chemically bound in the crystal structures of calcium hydroxide, calcium silicate hydrates (C-S-H), calcium alumino-ferrite hydrates, and calcium sulfate and aluminosulfate phases.[5] Water that is not chemically bound is referred to as free water[6] and is characterized as follows:

1) Water physically bound (sorbed) on to the surfaces of the hydrated phases. This water is located in the gel pores (radii up to 5nm) and is referred to as gel water.

2) Water chemically sorbed in the interlayer spaces between the C-S-H sheet structures. This water is referred to as structural water. (Some classifications include this water with the gel water.)

3) Water present in the capillary pores. The transition between gel pores and capillary pores is not sharp.

4) Water may also be sorbed on the surfaces of larger pores formed by entrapped air, entrained air, or poor compaction or fracture surfaces. Non air-entrained concrete contains 1-2 volume percent air incorporated as part of the manufacturing process.

This general description of porosity and water content is based on several models developed to describe the general structure of cement paste and to approximate the microstructure of hardened concrete [Powers, 1958, Feldman and Sereda, 1968, Wittmann, 1968]. These models used measurements of total water, evaporable water and water vapor sorption isotherms, or N_2 sorption isotherms to differentiate between bound water, capillary

---

[3] A gel is a colloidal suspension of a liquid in a solid.

[4] The porosity of the interfacial zone between the paste and aggregate in some cases can contribute significantly to the overall porosity. Tensile stress between still aggregate and less stiff cement paste can also cause micro cracking and porosity.

[5] Cement notation is used to represent oxides in chemical formulas and equations. A = Al_2O_3, C = CaO, F = Fe_2O_3, H = H_2O, K = K_2O, M = MgO, N = Na_2O, P = PO_4, S = SiO_2, $\bar{S}$ = SO_4.

[6] Free water is water that evaporates below 100C, i.e. in response to changes in relative humidity at ambient conditions.

water and gel water.[7] Schematic representations of the Feldman-Sereda model and the Munich model are presented in Figure 3-1 (a, b, respectively).

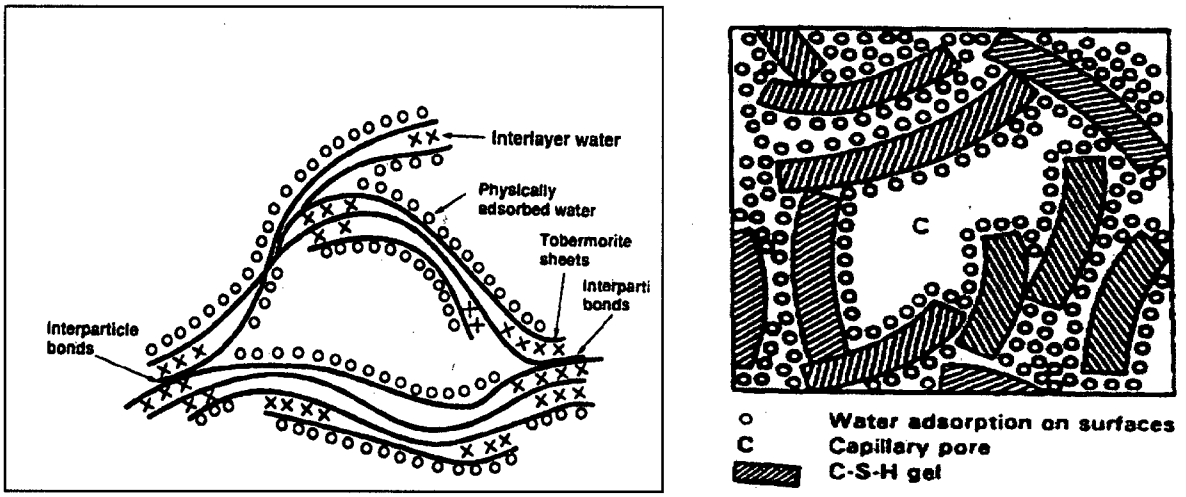

Figure 3-1. Microstructure models for hardened Cement Paste (a) Feldman-Sereda Model, (b) Munich Model.

Details of the cement paste microstructure models are reviewed elsewhere [Taylor, 1997]. Taylor, 1997, used the Powers-Brownyard Model to calculate the relationship between gel and capillary porosities as a function of curing time (fraction of hydrated cement) and water to cement ratio. The results of these calculations are shown in Table 3-1 and apply to portland cement paste. The relationships between the solid hydration products, gel pores and capillary pores as a function of water to cement ratio for fully hydrated cement paste is illustrated in Figure 3-2.

3.1.1 Blended Cements Pore Structures

The same general pore structure relationships that apply to portland cement pastes also apply to blended cements which contain slag cement, fly ash, and other pozzolans in combination with portland cement. However, for substitutions of pozzolan beyond that which is required for complete reaction with portlandite, the hydrated fraction and the volume fractions of the hydrated products must be determined experimentally. For example the porosity of the 14 month old blended pastes was found to be higher than the porosity of Portland cement paste with the same water to cement ratio and curing time [Harrisson, 1987 and Taylor 1987].

[7] The Wittman model (Munich model) describes the microstructure as a xero-gel, a gel from which the dispersion medium is absent and was used primarily in the development of a theory of dimensional changes.

The higher porosities observed in the blended cement pastes are the result of less hydration products formed in these mixtures. For example, fly ash in 14 month old cement paste will only be partially hydrated. See data provided in Table 3-2 [Taylor 1987, Harrisson, 1987]. This effect increases with the percentage replacement and is especially marked at early ages. On the other hand slag cement hydrates to the C-S-H and a hydrotalcite-type phase which tends to lower the porosity. Silica fume hydration also lowers porosity.

Table 3-1. Calculated porosities for cement pastes based on the Powers-Brownyard Model and Parrott and Killoh calculations [after Taylor, 1997].

w/c	Fraction of Cement Hydrated	Capillary Porosity (volume fraction)	Gel Porosity (volume fraction)	Total Porosity (volume fraction)
0.3	0.00	0.49	0.00	0.49
0.3	0.79	0.00	0.27	0.27
0.35*	*1.00*	*0.07*	*Not Recorded*	*Not Recorded*
0.4	0.00	0.56	0.00	0.56
0.4	1.00	0.03	0.29	0.32
0.5	0.00	0.61	0.00	0.61
0.5	1.00	0.15	0.26	0.41
0.5*	*1.00*	*0.16*	*Not Recorded*	*Not Recorded*
0.6	0.00	0.65	0.00	0.65
0.6	1.00	0.24	0.23	0.47
0.65*	*100*	*0.26*	*Not Recorded*	*Not Recorded*

* [Parrott 1981]. Reported as the fraction of pores >4nm in mature cement pastes.

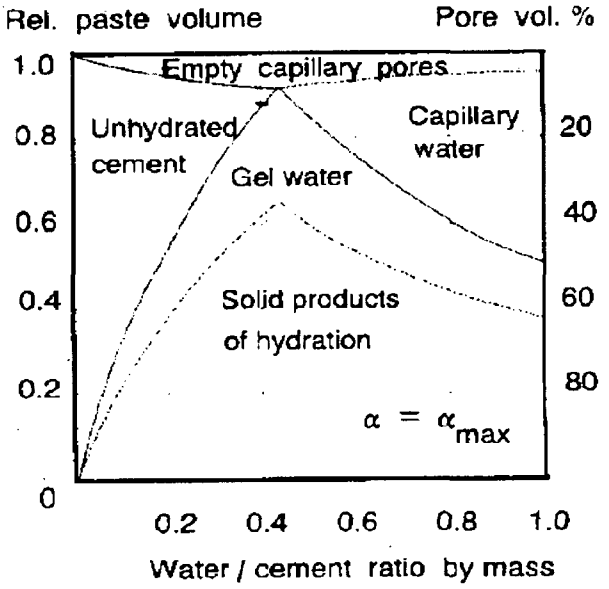

Figure 3-2. Volume fractions of the various phases in completely hydrated cement paste [Reinhardt, 1992].

Table 3-2. Effects of mineral additions on porosity for blended cements.

Material	Capillary Porosity Porosity realized by equilibrating paste at 11 and 90 % RH (vol %)	Porosity of the Free Water (All bound water; gel and interlayer water) (vol %)
Portland cement paste w/c = 0.5 [Taylor 1987]	19	29
Blended Portland cement paste with 40% slag replacement Blended cement paste with 20 % fly ash replacement [Harrisson, 1987]	22	34

3.1.2 Pore Connectivity

Powers used the water characterization and degree of hydration data described above to estimate the development of the microstructure as a function of the water to cement ratio and curing time. The approximate ages required to produce discontinuity (segmentation) in the capillary pores are summarized in Table 3-3 [Powers, 1958 and 1959]. This analysis assumes hydration under moist conditions to support full hydration and is for portland cement paste.

The methodology can be applied to blended cement pastes but the times to achieve discontinuity and the w/c threshold value for discontinuity will depend on the composition and properties of the specific blended cement system.

Table 3-3. Approximate age required to produce segmentation of the capillaries in cement paste [Powers, 1958].

w/c	Time required to achieve capillary discontinuity
0.40	3 days
0.45	7 days
0.50	14 days
0.60	6 months
0.70	1 year
> 0.70	Impossible

Garboczi and Benzt modeled hydration of tricalcium silicate and determined that when the capillary porosity reached about 18 volume percent, the capillary pore system becomes

discontinuous [Garboczi and Bentz, 1989]. The same relationship is expected to apply to Portland cement pastes. See Figure 3.3.

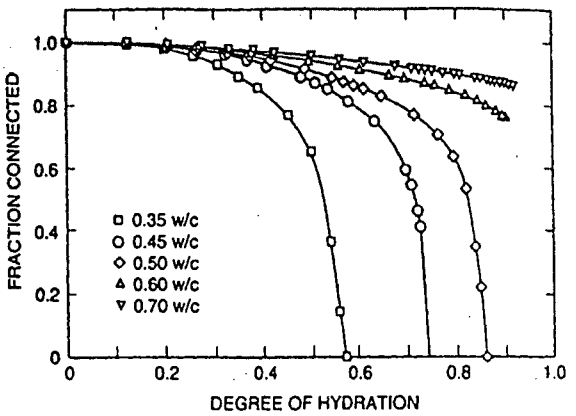

Figure 3-3. Connected capillary porosity versus degree of hydration [Garboczi and Bentz, 1989].

In summary, if non porous aggregates are used, the total porosity in concrete is the sum of the pores in the hydrated cement paste plus voids (1-2 volume percent minimum air voids). The total porosity typically ranges from 10 to 20 volume percent depending on the water to cement ratio, cement content and degree of hydration. The continuity of the capillary pores depends on the water to cement ratio and the degree of hydration. Below a water to cement ratio of about 0.6 the capillary pore structure is discontinuous. At higher water to cement ratios, the larger capillary pores and a portion of the small capillary pores are continuous.

The pore-size distribution of a cement mortar sample (impermeable sand) is provided in Figure 3-4 to illustrate the very fine structure of cement paste. Connectivity of the larger pores is typically through smaller pores.

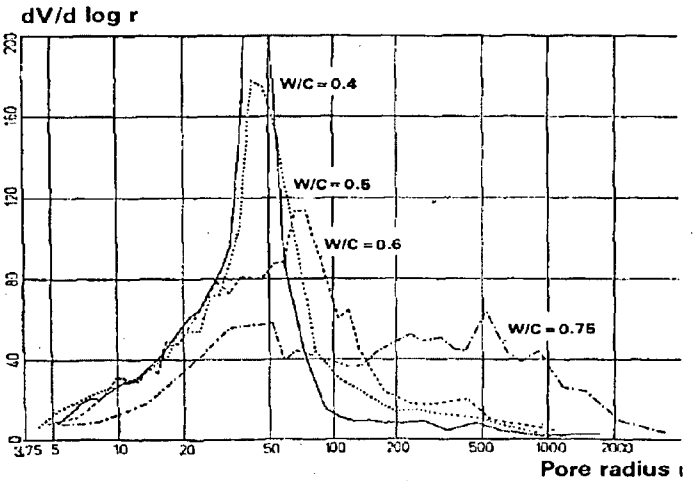

Figure 3-4. Pore size distribution of cement mortar. Pore radii in nm. [Reinhart, 2002].

3.2 Relationship between Pore Structure and Transport Phenomena

The rate of water, gas, and ion transport through the material are controlled by the microstructure and binding capacity of the material. Numerous representations of the relationship between water, gas and ions transport through concrete and the pore structure have been published [Bakker, 1983, Nyame, 1981, Hughes, 1985, Roy, 1993]. A simple porosity-permeation model by Hearn and Figg, 2001, is provided in Figure 3-5 and represents the basic transport mechanisms that are relevant to cementitious materials.

	System 1	System 2	System 3
Continuous pore radius	Large	Medium	Small
			
Pore sizes (μm)	10–100	0.1–10	0.001–0.1
Controlling transmission mechanisms	Darcian flow Ionic diffusion	Capillary suction Evaporation Ionic diffusion	Vapor diffusion

Figure 3-5. Schematic representation of cement pore structures and transport mechanisms [Hearn and Figg, 2001].

The general relationship between water permeability and porosity as a function of water to cement ratio and degree of hydration is illustrated in Figure 3-6.[8]

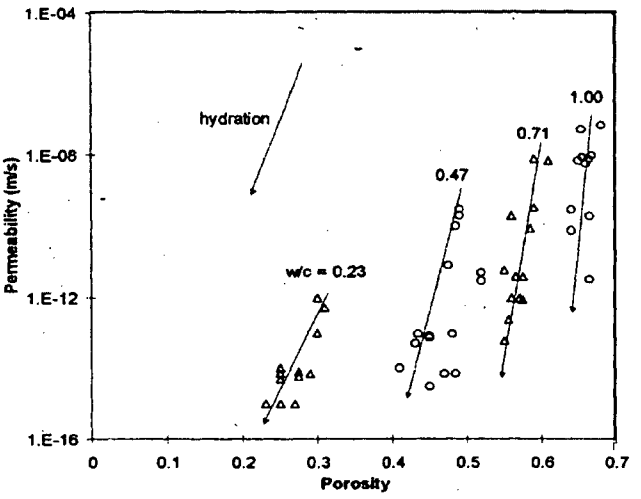

Figure 3-6. Relationship between porosity and permeability as a function of w/c and hydration [Nyame, 1981].

[8] The Darcian permeability of C-S-H gel was calculated by Powers to be 2×10^{-17} m/s. This value is considered to be the limiting permeability of hydrated portland cement systems [Powers, 1959].

3.3 Degradation of the Pore Structure and Relation to Transport Properties

Under field conditions, concrete is exposed to a combination of physical and chemical processes. Some processes are beneficial (continuing hydration, self sealing, carbonate sealing, tightening of the microstructure due to expansion under compression) while others create irreversible deleterious changes at early stages (shrinkage, thermal cracking) or after the material is aged (excessive loading or chemical attack such as rebar corrosion, decalcification, etc.). All of these processes modify the hydrated paste pore structure and/or result in cracks.

Transport processes, (Darcian flow or advection, ionic, moisture, and gas diffusion, capillary suction and evaporation) are the same for intact and degraded material. The relative contribution to transport changes as connected porosity increases through leaching and cracking. Some effects of generic degradation processes are listed in Table 3-4.

Table 3-4. Effects of generic degradation processes.

Process	Effect on pores and pore structure
Aging Continued hydration	Capillary pores converted to gel pores Reduction in pore connectivity
Mass Gain	Surface armoring Pore plugging Crack healing
Expansion Expansive phase formation	Cracking Spalling (reduction in thickness)
Mass Loss Leaching	Pore / Crack widening and increased connectivity
Mechanical Forces	Cracking Displacements

3.4 Concrete Degradation Modeling

Engineers are increasingly using numerical models to predict the service life of concrete structures exposed to a variety of conditions. These tools are used by designers and project managers to evaluate the impacts of various factors such as concrete mix characteristics, concrete cover, and protective surface treatments, on the service life of new and existing concrete structures. The materials science underlying these models is summarized below.

Structural degradation of concrete is controlled by transport of ionic species and moisture. Early ionic transport models were limited to simplified equations describing the diffusion of a single ion in saturated concrete. Over the past 30 years, service life modeling has evolved to account for the complexity of ionic transport in saturated and unsaturated systems and consider diffusion and other transport mechanisms such as water movement under the effect of humidity gradients.

Ionic transfer models (typically finite element models) for concrete and reviews of modeling methodology are provided elsewhere [Luping, 2001, Maekawa, 2001, Henchi, 2007, Samson, 2001 and 2006, Glasser, 2007]. A general description of the parameters and approaches for modeling ionic and moisture transport are summarized below [after Glasser, 2007]:

- Ionic transport phenomena are typically described by writing mass conservation equations at the pore scale.
  - At the pore scale, ionic transport is assumed to be controlled by an electrochemical potential gradient and advection. The electrochemical potential of each ionic species can be described by terms for diffusion, electrical potential, activity, and temperature dependency of the activity. Each of these terms can be further defined. For example, the diffusivity of each ion through the concrete is a function of diffusion coefficient in free water, tortuosity, degree of saturation of the concrete pores, activation energy, and a correction factor to account for chemical reactions.

  - Many ionic models neglect the electrochemical potential and electrical coupling between ions. This is the case in routine groundwater modeling where the ionic concentrations are relatively low. However, for cement pore solutions with high concentrations of dissolved species, strong concentration gradients result in electrochemical potential terms that are not negligible. Recent developments in this area have been applied to modeling ionic transport in concrete [Truc, 2000, Masi, 1997].

- Modeling transport at the pore scale is not possible for technical and computational reasons. To overcome these difficulties several approaches have been applied and tested. Two are mentioned below:
  - Pore- scale equations can be averaged over the scale of the material using a mathematical technique referred to as homogenization. This technique was applied by Samson, et al. and the approach was referred to as the Representative Elementary Volume technique [Samson, 2005]. By solving the averaged mass transport equations, one can perform simulations at the scale of the concrete structure or element.
  - Johannessson overcame this problem by using mixture theory [Johannesson 2003].

- Two main approaches have been used to model moisture movement in hydrated cement systems.
  - One system is based on a detailed description of all of the phases involved in the process: liquid, water vapor, and dry air. Multiple mass conservation equations are used to obtain a description of the "global moisture fields" [Mainguy, 2001, Selih, 1996]. This approach is marginally useful for durability evaluations because of the large number of parameters that need to be determined [Taylor, 2007].

- A simplified approach can be derived from the first using assumptions and results in a single equation (Richards' Equation) and is often selected to describe the variation in water content within cementitious materials. One of the main differences between the two approaches is the assumption that gas pressure is uniform over the material and is equal to atmospheric pressure.
  - Applicability of the Richards' equation for describing the water content of concrete has been demonstrated [Samson, 2005].
  - Instead of using water content as a variable of state, other authors have chosen to use the relative humidity field [Bazant, 1971, Xi, 1994].

The most advanced multi ionic models for concrete service life prediction incorporate the effects of ionic coupling, wet-dry cycling, temperature variations and multiple chemical reactions that account for dissolution and precipitation. STADIUM®, which was developed by SIMCO Technologies, Inc., is an example of a commercially available advanced multi ionic model developed for concrete service life [Samson, 2007]. [9]

Comprehensive characterization of the concrete microstructure, pore solution chemistry, moisture and ionic diffusion coefficients and exposure conditions is required to support the advanced simulations used to predict concrete service life.

3.5 References

Bakker, R.F.M, 1983. "Permeability of Blended Cement Concretes, ACI-SP-70, Vol. 2, V.M. Malhotra, Ed., p.589-605.

Bazant, Z.P. and L.J. Najjar, 1971. "Drying of Concrete as a Nonlinear Diffusion Problem," *Cement and Concrete Research*, **34**, p.1859-1872.

Feldman, R.F. and P.J. Sereda, 1968. "A Model for Hydrated Portland Cement Paste As Deducted from Sorption-Length Change and Mechanical Properties," Material Structures, **1**[6], p. 509-520.1968.

Garboczi, E.J. and D.P. Bentz, 1989. "Fundamental Computer Simulation Models for Cement-Based Materials," p. 249-277, Materials Science of Concrete II, J. Skalny and S. Mindess Eds., American Ceramic Society, Westerville, OH, 1989.

Glasser, F. P., J. Marchand and E. Samson, 2007. "Durability of Concrete – Degradation Phenomena Involving Detrimental Chemical Reactions, Key note address, 2007.

Harrisson, A.M., N.B. Winter, and H.F.W Taylor, 1987. J. Material Sci. Let. **6**, p. 1339.

Hearn, N. and J. Figg, 2001. "Transport Mechanisms and Damage: Current Issues in Permeation Characteristics of Concrete," p. 327-375, Materials Science of Concrete VI, S. Mindess and J. Skalny, Eds., American Ceramic Society, Westerville, OH, 2001.

[9] Service life predictions using the STADIUM model have been tested and verified for in-service concrete structures [Samson, 2007]

Henchi, K., E. Samson, F. Chapdelaine, and J. Marchand, "Advanced Finite Element Predictive Model for the Service Life Prediction of Concrete Infrastructures in Support of Assessment Management and Decision Making," provided through personal communication, 2007.

Hugnes, D.C., 1985. "Pore Structure and Permeability of Hardened Cement Paste," *Mag. of Concrete Research*, 37[133], p.227-233. Check C&CR 15, p1003, 1985

Johannesson, B.F., 2003. "A Theoretical Model Describing Diffusion of a Mixture of Different Types of Ions in Pore Solution of Concrete Coupled to Moisture Transport," *Cement and Concrete Research*, **33**, p.481-488.

Lupig, T. and L.O. Nilsson., 1993. "Chloride Binding Capacity and Binding Isotherms of OPC Pastes and Mortars," *Cement and Concrete Research,* **23**, p.247-253. 1993.

Maekawa, K. and T. Ishida, 2001. "Service –Life Evaluation of Reinforced Concrete Under Coupled Forces and Environmental Actions, Ion and Mass Transport in Cement-based Materials, Materials Science of Concrete, Special Vol., R.D. Hooton, M.D.A. Thomas, J. Marchand, and J. Beaudoin, Eds., p. 219-238, American Ceramic Society, Westerville, OH, 2001.

Mainguy, M., O. Coussy, and V. Baroghel-Bouny, 2001. "Role of Air Pressure in Drying of Weakly Permeable Materials, *J. Engineering Mechanics*, **127**, p.582-592.

Masi, M., D. Colella, G. Radaelli, and L. Bertolini, 1997. "Simulaion of Chloride Penetration in Cement-Based Materials," *Cement and Concrete Research* **27**, p.1591-1601, 1997.

Mindess, S. and J.F. Young, 1981. Concrete, Prentice Hall Inc., NY, 1981.

Nyame, B.K. and J.M. Illston, 1981. "Relationship Between Permeability and Pore Structure of Hardened Cement Paste," Magazine of Concrete Research, **33**[116]. p.139-146.

Parrott, L. J., 1981. *Cement and Concrete Research*, **11**, p.651.

Powers, T.C. and T.L.Brownyard, 1948. "Studies of Physical Properties of Hardened Portland Cement Paste," R&D Bulletin 22, Portland Cement Association, Skokie, IL, 1948.

Powers, T.C. 1958. "Structure and Physical Properties of Hardened Portland Cement Paste," J. Am. Ceramic Soc., **41**, p.1-6, 1958.

Powers, T.C., L.E. Copeland, and H.M. Mann, 1959. "Capillary Continuity or Discontinuity in Cement Paste," J. Portland Cement Association, **1**[2], p.38-48, 1959.

Reinhardt, H.W., 2002. "Transport of Chemicals Through Concrete," p.209-241, Materials Science of Concrete III, J. Skalny, Ed., American Ceramic Society, Westerville, OH, 2002.

Roy, D.M., P.W. Brown, D. Shi, B.E. Scheetz, and W. May, 1993. "Concrete Microstructure Porosity and Permeability," SHRP-C-628, Strategic Highway Research Program, National Research Council, Washington DC.

Samson, E., J. Marchand and Y. Maltais. "Modeling Ionic Diffusion Mechanisms in Saturated Cement-Based Materials – An Overview," Ion and Mass Transport in Cement-based Materials, Materials Science of Concrete, Special Vol., R.D. Hooton, M.D.A. Thomas, J. Marchand, and J. Beaudoin, Eds., p.97-111, American Ceramic Society, Westerville, OH, 2001.

Samson, E., J. Marchand, K.A. Snyder, and J.J. Beaudoin, 2005. "Modeling Ion and Fluid Transport in Unsaturated Cement Systems in Isothermal Conditions," *Cement and Concrete Research*, **35,** p.141-153.

Samson, E. and J. Marchand, 2006. "Modeling the Effect of Temperature on Ionic Transport in Cementitious Materials," *Cement and Concrete Research*, **36**, p. 455-468.

Samson, E. 2007. Personal communication in support of the DOE-EM sponsored Cementitious Barrier Partnership.

Selih, J. A.C.M. Sousa, and T.W. Bremmer, 1996. "Moisture Transport in Initially Fully Saturated Concrete During Drying." *Transport in Porous Media,* **24,** p.81-106.

Taylor, H.F.W., 1987. Materials Research Soc. Symp, Proc. **85**, p.47.

Taylor, H. F. W., 1997. Cement Chemistry, p. 231-259, Thomas Telford, London, 1997.

Truc, O., J.P.Ollivier, and L.O. Nilsson, 2000. "Numerical Simulations of Multi-Species Diffusion," *Materials and Structures* **33**, p.566-573.

Wittman, F.H. and G. Englert, 1968. "Water in Hardened Cement Paste," *Material Structures*, **1**[6], p.535-546, 1968.

Xi, U, Z.P. Baxant, L. Molina, and H. M. Jennings, 1994. "Moisture Diffusion in Cementitious Materials – Moisture Capacity and Diffusivity," Advanced Cement Based Materials, **1**, p.258-266.

4.0 REVIEW OF CHEMICAL DEGRADATION MECHANISMS

4.1 Degradation Overview

Service life assessments of concrete structures are primarily concerned with premature failure of the mechanical properties of the structure. In contrast Performance Assessments of low level waste (LLW) cementitious barriers are primarily concerned with the evolution of chemical and hydraulic properties of the cementitious barriers, and the resulting impacts on the flux of radionuclides at the barrier-environment boundary and point of compliance.

Structural failure can be caused by mechanical stresses such as, overload, creep, or seismic events and/or by chemical processes which reduce the strength of the material. This report is limited to chemical degradation processes that may affect subsurface cementitious barriers used in the disposal of radioactive waste.

Chemical degradation is controlled by movement of water and dissolved ions through concrete and is illustrated in Figure 4-1. The rate of transport of moisture and ions is a function of pore structure of the cement matrix as described in Section 3. Cracks resulting from one or more degradation processes increase the over all transport of moisture and dissolved ions through the concrete and consequently accelerate the deterioration cycle.

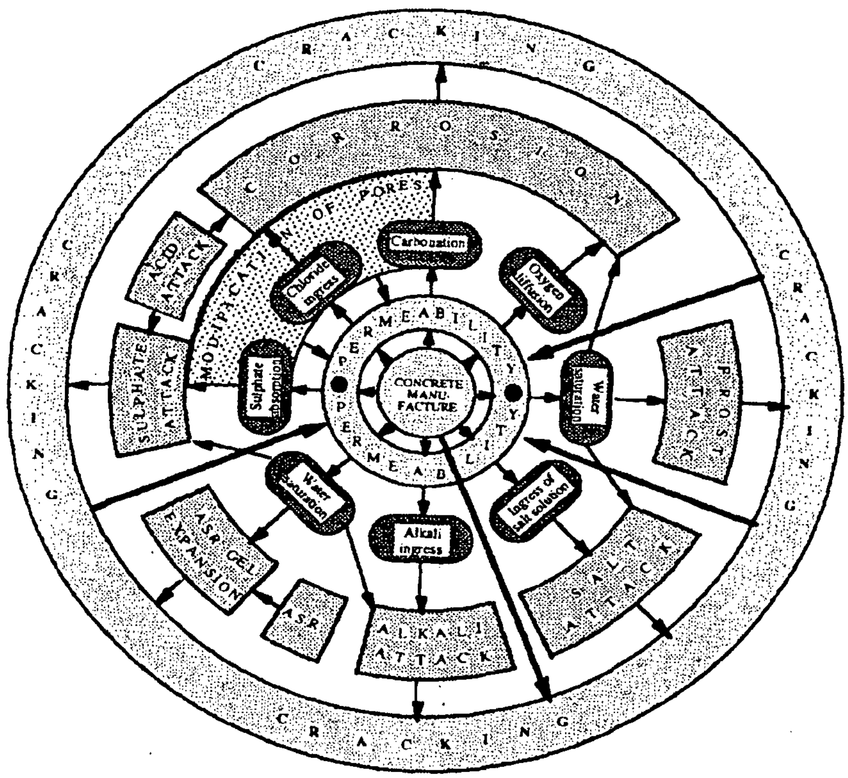

Figure 4-1. Relationship between pore structure (represented by permeability) and deterioration [Long, 1997].

In service, concrete and cementitious barriers are exposed to both chemical and physical processes. Some processes are beneficial such as continued hydration and carbonation of non reinforced cementitious material.[10] Other processes damage the microstructure (increase porosity and permeability) and/or result in cracks. Cracks can be classified based on cause as illustrated in Figure 4-2.

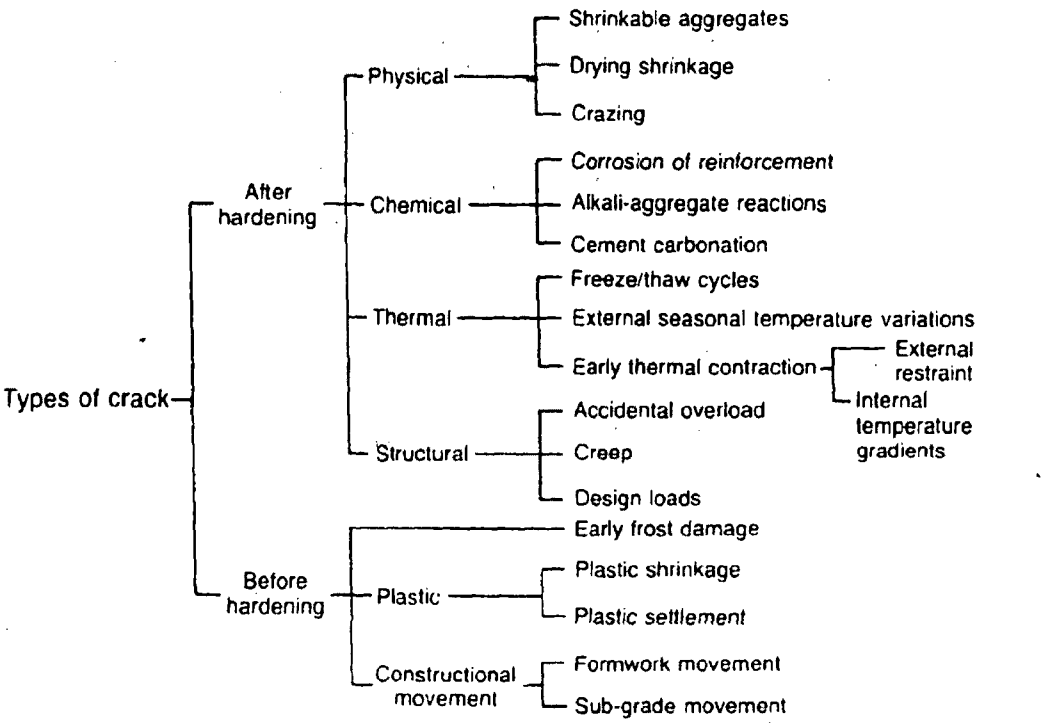

Figure 4-2. Crack classification based on various deterioration mechanisms [Cimite Euro-International du Beton, 1992 (after Hearn, 2001)].

Chemical degradation mechanisms discussed in this report are acid attack (decalcification), carbonation, sulfate attack, alkali aggregate reaction, and reinforcing steel corrosion. These processes result in an increase in porosity and cracking. Cracking associated with wet-dry cycling and freeze thaw cycling were not discussed because the cementitious barriers in the F-Tank Farm closure concept will be located in the sub surface environment and will not be subjected to these conditions.

[10] Carbonation results in precipitation of calcium carbonate which can plug pores or seal the surface of a affected concrete. Carbonation can also have detrimental effects such as lowering of alkalinity of the barrier which may have a negative consequence for leaching of certain ions and carbonation-induced rebar corrosion.

Structural degradation (cracking) in response to thermo mechanical forces was not considered in this analysis. However the FTF PA analysis does include fast pathways [Rosenberger, 2007]. The response of degraded material to mechanical forces is also not considered in this report.[11]

Cementitious barriers used for LLW isolation have additional chemical durability requirements involving pH and Eh of the barrier system (CO_2 and O_2, respectively). The effects of chemical reactions which result in changes in oxidation state and pH on contaminant leaching are described elsewhere [Kaplan, 2006 and 2007 (a), (b), (c) respectively, Denham, 2007]

4.1.1 References

Denham, M.E., 2007. "Conceptual Model of Waste Release from the Contaminated Zone of Closed F-Area Tanks," WSRC-STI-2007-00544, September 2007, Washington Savannah River Company, Aiken SC 29808.

Hearn, N. and J. Figg, 2001. "Transport Mechanisms and Damage: Current Issues in Permeation Characteristics of Concrete," p. 327-375, Materials Science of Concrete VI, S. Mindess and J. Skalny, Eds., American Ceramic Society, Westerville, OH, 2001.

Kaplan, D. I., 2006. "Geochemical data Package for Performance Assessment Calculations Related to the Savannah River Site (U)," SRC-TR-2006-00004 Rev.0, February 28, 2006, Washington Savannah River Company, Aiken SC 29808.

Kaplan, D. I., 2007. "Distribution Coefficients for Various Elements of Concern to the Tank Waste Performance Assessment," SRNL-RPA-2007-00006, July 10, 2007, Washington Savannah River Company, Aiken SC 29808.

Kaplan, D. I., 2007. "Subject: K_d Values," E-mail to R. Cauthen, July 16, 2007, Washington Savannah River Company, Aiken SC 29808.

Kaplan, D. I., 2007. "Concrete K_d Values Appropriate for the Tank Closure Performance Assessment," SRNL-RP-2007-01122, October 11, 2007, Washington Savannah River Company, Aiken SC 29808.

Long, A.E., P.A.M. Basheer, and F. R. Montgomery, 1997. "In-Situ Permeability Testing – A Basis for Service Life Prediction," p.651-670, in Advances in Concrete Technology Proceedings of the 3rd CANMET/ACI International Conference, Auckland, New Zealand, 1997.

Rosenberger, K.H., 2007, Personal communication with C.A. Langton.

[11] It is assumed that the response of a degraded structure to overload, creep, and/or seismic events will be more severe than that of an intact structure.

4.2 Decalcification (Acid Attack)

4.2.1 Description and Mechanism

Decalcification of the calcium containing phases in hydrated portland cement paste plays a role in most of the chemical degradation processes affecting pastes and composite cementitious building materials (concrete, grout). Decalcification[12] refers to:

- Leaching of calcium ions (coupled with hydroxide ions) from pore solution of cementitious materials, and
- Dissolution of calcium hydroxide, C-S-H, and hydrated calcium aluminate phases in cementitious materials.[13]

Decalcification is also referred to as acid attack. The processes and consequences of decalcification are shown in Figure 4-3.

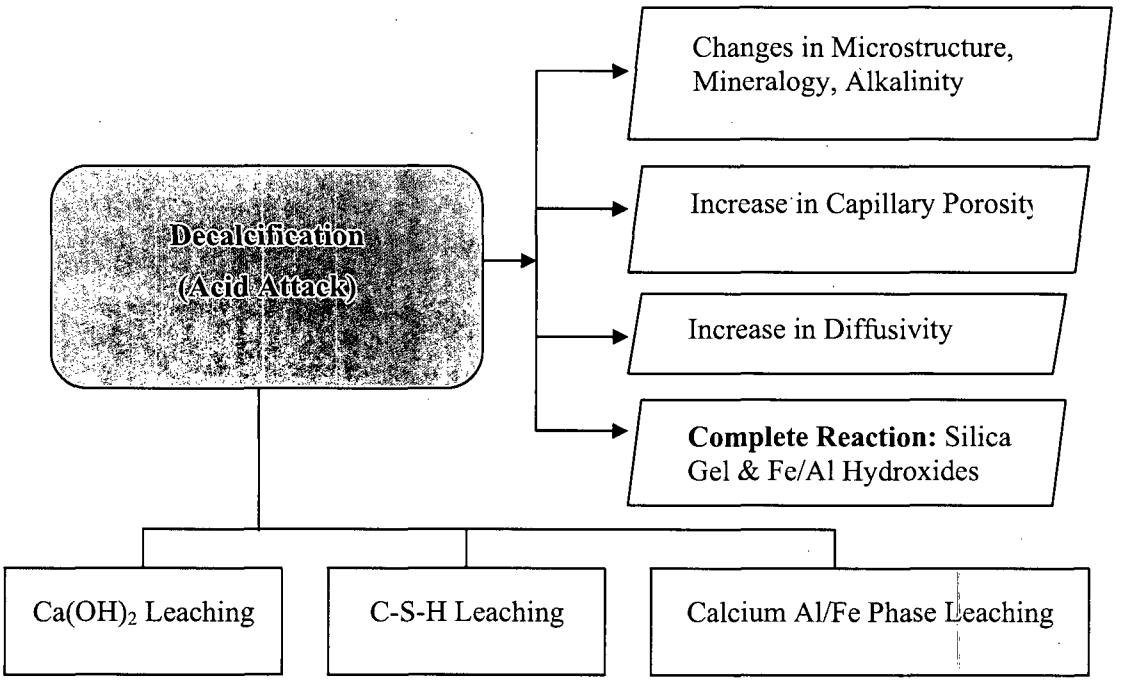

Figure 4-3. Decalcification (Acid Attack) processes and consequences.

[12] Decalcification also includes leaching of alkali ions (K^+ and Na^+) from the cementitious material.

[13] Adenot showed that the first phase to disappear from the exposed surface was calcium hydroxide, followed by the monosulfate, AFm phase, then ettringite, and then C-S-H. Although C-S-H was the last to disappear it was progressively decalcified as a function of exposure [Abenot,1992]. The longer persistence of ettringite compared to monosulfate is consistent with the observation that monosulfate is not stable at or below pH of 11.6, whereas, ettringite decomposes below a pH of 10.7 [Gabrisova, 1991]

Acid Attack. This form of degradation typically affects concrete structures in contact with acidic flowing or percolating acidic water for long periods of time. The removal of calcium from the matrix material decreases its strength and increases permeability. The ultimate residue produced by decalcification consists of hydrous forms of silica (silica gel), alumina (alumina gel) and iron oxide. Attack is most serious with pure water and acidic water.

Leaching creates Ca^{+2} and OH^- concentration gradients across the affected region (exposed surface to unaffected material). These gradients result in diffusion of calcium and hydroxide ions in the pore solution from high to low concentrations and incongruent dissolution (decalcification) of the calcium-containing phases.

The physical consequence of this process is a multi-layer degraded zone. The various layers are separated by dissolution and precipitation fronts and are characterized by specific mineral assemblages [Adenot, 1992, Herold, 1997, Faucom, 1997, Carde, 1997]. Decalcification changes the bulk density and the pore structure of the affected cementitious material. The consequences are an increase of the porosity and permeability, and a loss of mechanical strength.

The rate of attack depends on the flow rate and chemistry of the water contacting the cementitious material, temperature, and whether the water flows through or over the material. The rate of attack also depends on the availability of calcium hydroxide in the cementitious material. Materials containing blended cements, slag cement or pozzolans such as fly ash in addition to portland cement, have less available $Ca(OH)_2$ than neat portland cements, and, therefore, experience a slower rate of leaching all other things being equal.

4.2.2 Models for Acid Attack (Calcium Hydroxide Leaching)

Decalcification is a coupled dissolution/diffusion process. The simplest approach for simulating acid leaching is to assume a diffusion controlled process. The description of ionic transport phenomena at the pore scale has advanced considerably over the last ten years. Most simulate acid attack as leaching of calcium hydroxide from the matrix. Some of these models also take into account the evolution of the porosity as the solid phases dissolves [Delagrave, 1997, Marchand, 2001, Maltais 2004, and Haga, 2005].

Marchand, et al., 2001, investigated the influence of calcium hydroxide dissolution and its effects on the diffusion properties of three different hydrated cement pastes at two different water to cement ratios. He used the National Institute of Standards and Testing (NIST) CEMHYD3D® cement hydration and microstructure development model. The results of these simulations were implemented in another numerical model, STADIUM® to predict the transport of ions in unsaturated porous system.

These numerical simulations indicated that calcium hydroxide dissolution contributes to a marked increase in porosity of the hydrated cement paste. The predicted results were in good agreement with experimental data obtained from leaching experiments performed in deionized water.

INEEL Tank Closure PA Approach. A simple diffusion model was used in the INEEL PA to simulate the depth of penetration and the volume of affected material for degradation by acid leaching [INEEL Appendix E, 2003]. This model is based on work Walton, et al., 1990 who summarized modeling and experimental results from Atkinson, et al., 1985 and from the Barrier Code which was an early model for predicting the long term performance of concrete [Shuman, R., V.C. Rogers, and R. A. Shaw, 1989].

In this model calcium removal from the exposed surface was assumed to be rapid compared to the transport via diffusion of calcium through the pore solution in the material. Therefore the concentration of calcium was assumed to be zero at the surface. The model did not take into account phase and microstructural changes that accompany decalcification.

A four-stage calcium leaching process was assumed based on experimental work of the time dependence of pH in a repository containing cementitious material [Atkinson, 1985 and 1988]. The stages are:

1. The initial pH is approximately 13 and is controlled by alkali metal hydroxides which are the first components to be leached.
2. The pH falls to 12.5 and is controlled by $Ca(OH)_2$ dissolution equilibria as shown below:

$$Ca(OH)_2 \longrightarrow Ca^{2+} + 2OH^-$$

3. The pH slowly falls to 10.5 as C-S-H phases begin to dissolve incongruently after the calcium hydroxide is depleted.
4. The pH is held at 10.5 by congruent dissolution of C-S-H.

In the INEEL shrinking core diffusion model, depletion took place from the outer surface inward to the core. The radius of the cylindrical unleached zone decreases over time as calcium was removed from the surface. The radius of the unleached zone is described in Equation 1.

Equation 1. $$X = \left(2D\tau\Phi \frac{(C_l - C_{gw})t}{C_s} \right)^{1/2}$$

The leaching process is assumed to be controlled by diffusion and was described as a molar out flux of Ca. The flux is described in Equation 2.

Equation 2. $$X = -D\tau\Phi \frac{(C_l - C_{gw})}{R}$$

The change in the radius of the unleached zone is described in equation 3. The thickness of the leached zone is R_0- R.

Equation 3. $$\frac{dX}{dt} = \frac{D\tau\Phi C_l}{RC_s}$$

where:

C_l = Concentration of Ca^{2+} ions in the concrete pores (moles/cm^3)
C_s = Bulk concentration of Ca^{2+} ions in the solid concrete (moles/cm^3)
C_{gw} = Concentration of Ca^{2+} ions in the soil pore water (conservatively assumed to be zero (moles/cm^3)
D = Diffusion coefficient of Ca^{2+} ions in concrete (cm^2/s)
X = Distance (penetration) in concrete (cm)
N = Molar flux (moles/cm^2/sec
t = Time (s)
τ = Tortuosity factor
Φ = Porosity (volume assumed to be saturated)

4.2.3 References Calcium Hydroxide Leaching

Adenot, F. and M. Buil, 1992. "Modeling of the Corrosion of the Cement Paste by Deionized Water," *Cement and Concrete Research*, **22**[2/3], p.489-496, 1992.

Atkinson, A, D.J. Goult, and J. A. Hearne, 1985. "An Assessment of the Long-Term Durability of Concete in Radioactive Waste Repositories," Materials Research Society, **50**, p. 239-246, 1985.

Carde, C., R. Francois and J-P. Ollivier, 1997. "Microstructural Changes and Mechanical Effects Due to the Leaching of Calcium Hydroxide from Cement Paste," p.30-37, Proceedings of the Materials research Society's Symposium on Mechanisms of Chemical Degradation of Cement-Based Systems, Boston, November 27-30, 1995, Published in Mechanisms of Chemical Degradation of Cement-Based Systems, Eds., K. L. Scrivener and J.F. Young, E&FN SPON, London, 1997.

Delagrave, A., B. Gerard, and J. Marchand, 1997. "Modeling the Calcium Leaching Mechanisms in Hydrated Cement Pastes," p.38-49, Proceedings of the Materials research Society's Symposium on Mechanisms of Chemical Degradation of Cement-Based Systems, Boston, November 27-30, 1995, Published in Mechanisms of Chemical Degradation of Cement-Based Systems, Eds., K. L. Scrivener and J.F. Young, E&FN SPON, London, 1997.

Faucon, P., F. Abendot, M. Jorda, and R. Cabrillac, 1997. "Behaviour of Crystallized Phases of Portland Cement Upon Water Attack," *Materials and Structures*, 30, p.480-485, 1997.

Glasser, F. P., J. Marchand and E. Samson, 2007. "Durability of Concrete – Degradation Phenomena Involving Detrimental Chemical Reactions, Key note address, 2007.

Gabrisova, A., J. Havlica, and S. Sahu, 1991. "Stability of Calcium Sulphoaluminate Hydrates in Water Solutions with Various pH Values," *Cement and Concrete Research*, **21**[6], p.1023-1034, 1991.

Haga, K.,S. Sutou, M. Hironaga, S. Tanaka, and S. Nagasaki, 2005. "Effects of Porosity on Leaching of Ca from Hardened Ordinary Portland Cement Paste," *Cement and Concrete Research*, **35**[9], p.1764-1775, 2005.

Herold, G., 1997. "Corrosion of Cementitious Materials in Acid Waters," p.98-105, Proceedings of the Materials research Society's Symposium on Mechanisms of Chemical Degradation of Cement-Based Systems, Boston, November 27-30, 1995, Published in Mechanisms of Chemical Degradation of Cement-Based Systems, Eds., K. L. Scrivener and J.F. Young, E&FN SPON, London, 1997.

INEEL PA Appendix E, 2003. "Degradation Analysis of the Grouted Tank/vault and Piping System at the Idaho Nuclear Technology and Engineering Center Tank Farm Facility and Preliminary Results for the Detailed Analysis of Releases from the Grouted Pipe and Encasement System, Revision 1,"p. E15, E20, INEEL, Idaho Falls, ID, 2003.

Maltais, Y., E. Samson, and J. Marchand, 2004. "Predicting the Durability of Portland Cement Systems in Aggressive Environments – Laboratory Validation," *Cement and Concrete Research*, **34**[9], p.1579-1589, 2004.

Marchand, J., D. P. Bentz, E. Samson, and Y. Maltais, 2001. "Influence of Calcium Hydroxide Dissolution on the Transport Properties of Hydrated Cement Systems," Materials Science of Concrete: Calcium Hydroxide in Concrete, Special Volume, Workshop on the Role of Calcium Hydroxide in Concrete, Proceedings, November 1-3, 2000, p.113-129, American Ceramic Society, 2001.

Revertegat, E., C. Richet and P. Gégout, 1992. "Effect of pH on the Durability of Cement Pastes," *Cement and Concrete Research*, **22**[2/3], p. 259-272, 1992.

Shuman, R., V.C. Rogers, and R.A. Shaw, 1989. "The Barrier Code for Predicting Long-Term Concrete Performance," Waste Management 89, University of Arizona, USA, 1989.

Taylor, H. F. W., 1997. Cement Chemistry, p. 380-381, Thomas Telford, London, 1997.

Walton, J.C., L.E. Plansky and R.W. Smith, 1990. "Models for Estimation of Service Life of Concrete Barriers in Low-Level Radioactive Waste Disposal," NUREG/CR—5542, TI91 000576, EG&G Idaho, Inc., Idaho Falls, ID 83415.

4.3 Carbonation – Special Case of Acid Attack

Carbonation is a special case of acid attack in which calcium is not leached from the material but is instead precipitated as calcite, $CaCO_3$. Transport of carbonate through concrete can occur as carbonate ion dissolved in water or as carbon dioxide in the vapor phase. Vapor phase diffusion is approximately four orders of magnitude more rapid than aqueous diffusion. Consequently carbonation rate is a function of saturation level and was found to be highest when the concrete has a relative humidity of about 50 % [Verbeck, 1958, Papadakis, et al. 1989].

Carbon dioxide in the air or dissolved in water reacts with the alkali and calcium ions in the pore solution of cementitious materials. Penetration of gaseous carbon dioxide into partially saturated portland cement-based materials initiates a series of chemical reactions involving the ions dissolved in the pore solutions and the solid hydrated phases. The process[14] is summarized below:

1. $CO_{2(g)}$ dissolves in pore solution as HCO_3^- and CO_3^{2-}. In portland cement-based materials which have alkaline pore solutions, CO_3^{2-} is the dominant species in solution.

$$CO_{2(aq)} + 2OH^- \longrightarrow CO_3^{2-} + H_2O$$

2. CO_3^{2-} reacts with dissolved calcium in the pore solution and calcite, $CaCO_3$, and calcium aluminate/silicate carbonate phases are precipitated.

$$Ca^{2+}(aq) + CO_3^{2-}(aq) \longrightarrow CaCO_3$$

3. The pH of the pore solution decreases as a result of these reactions. $Ca(OH)_2$ in the matrix continues to dissolve and buffer the pH of the pore solution back to 12.4 until the portlandite is consumed. The replacement of calcium hydroxide with calcite reduces the porosity of the material because calcite has a higher molar volume (36.9 cm/mol compared to 33.1cm^3/mole for portlandite)[15].

$$Ca(OH)_2 + CO_3^{2-}(aq) \longrightarrow CaCO_3 + 2OH^-$$

4. The process continues until all of the portlandite is dissolved. At this point, the dissolution chemistry is controlled by other hydrated calcium silicate and aluminate phases.

5. If carbonation continues to the final state, the resulting phases are silica gel (hydrated amorphous SiO_2, $Al(OH)_3$, $CaSO_4$ and hydrates, $CaCO_3$, and H_2O.

---

[14] For this mechanism of decalcification by acid leaching, the source of acid is assumed to be water in equilibrium with air (assuming a partial pressure of CO_2 in air at sea level of 32 Pa (10-3.5 atm).

[15] Molecular volume is the volume occupied by one mole. It is equal to the molecular weight divided by the density a phase.

The changes in pH of the pore solution due to carbonation are very abrupt and therefore are expressed as reaction fronts with discrete boundaries. Carbonation rate is a function of many variables including: microstructure and amount of Portland cement, which is the source of $Ca(OH)_2$.

Carbonation of reinforced concrete is expressed as rebar corrosion and results in serious structural degradation. The decrease in pH of the pore solution associated with the carbonation process has a detrimental effect on reinforced concrete structures by destroying the passive layer around the steel rebar. Rebar corrosion creates expansive forces at the rebar-concrete interface and is typically expressed as delamination of the surface cover and cracking parallel to the reinforcement. Iron staining on the exposed surface is the first indication of rebar corrosion. Carbonate induced rebar corrosion is discussed in Section 4.6, Reinforcing Steel Corrosion.

The carbonation process itself does not always have a negative effect on the cement paste properties or on un-reinforced concrete. Modification of the microstructure of hydrated portland cement paste, as measured by mercury intrusion porosimetry and water vapor sorption, indicates that the total porosity is always reduced by carbonation [Houst, 1997]. The effect of carbonation on the pore size distribution depends on the microstructure of the non-carbonated material (no steel reinforcement) and is strongly influenced by the water to cement ration and the composition of the cementitious material.

In the absence of other degradation mechanisms, carbonation, in itself, may be beneficial to the durability of the cementitious material since less porosity decreases the penetration of aggressive gases and solutions [Houst, 1997]. In some cases, carbonation can even form a protective layer on the surface of the cementitious material which reduces transport of soluble ions into and out of (leaching) the cementitious material [Garrabrants, 2006]. See Figure 4-4.

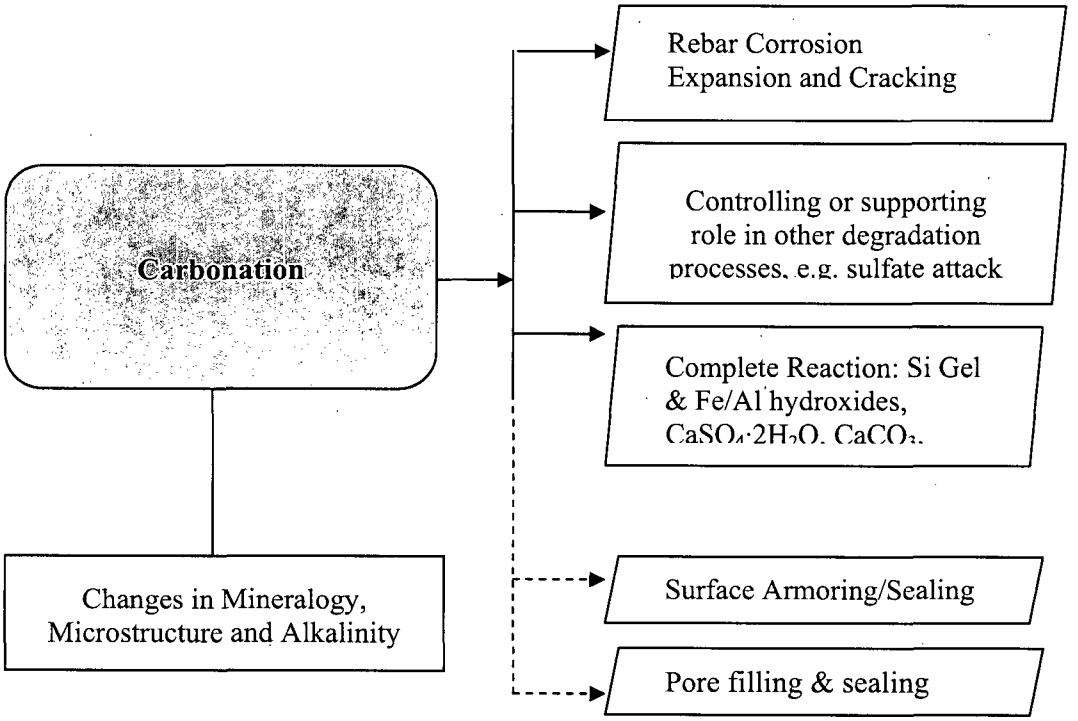

Figure 4-4. Carbonation processes and consequences.

4.3.1 Models for Carbonation.

Carbonation rate is often modeled as the depth of penetration of the carbonate by diffusion through the gas phase and is proportional to the square root of exposure time. The degree of saturation in the cement paste pores is important in determining the carbonate rate because CO_2 permeates the concrete most rapidly in the gas phase but the carbonation reactions take place in the liquid phase. Consequently, the most aggressive conditions of carbonation will occur when the pores have a layer of moisture on the walls but are not completely saturated (50-80% RH in the larger transmissive pores) [Verbeck, 1958, Papadakis, et al. 1989]. This condition satisfies the rapid transport of CO_2 through the gas phase and provides enough water for reaction. In completely saturated concrete, the CO_2 transport rate will be limited by initial dissolution in the pore solution and then diffusion of the ionic species through the pores to contact the alkaline phases.

More details on modeling carbonation are presented in the section on carbonate-induced rebar corrosion.

4.3.2 References for Carbonation

Garrabrants, 2007. Personal communication with C.A. Langton, 2007.

Houst, Y.F., 1997. "Microstructural Changes of Hydrated Cement Paste Due to Carbonization," p.90-97, Proceedings of the Materials research Society's Symposium on Mechanisms of Chemical Degradation of Cement-Based Systems, Boston, November 27-30, 1995, Published in Mechanisms of Chemical Degradation of Cement-Based Systems, Eds., K. L. Scrivener and J.F. Young, E&FN SPON, London, 1997.

Papadakis, V.G., C.G. Vayenas, and M. N. Fardis, 1989. "A Reaction Engineering Approach to the Problem of Concree Carbonation," AIChE J. **35**(10), p. 1639-1650, 1989.

Rosenberg, A. and C.M. Hansson, 1989. "Mechanisms of Corrosion of Steel in Concrete," Materials Science of Concrete Volume I, J. Skalny Ed., p. 285-313, American Ceramic Society, Westerville, OH, 1989.

Taylor, H. F. W., 1997. Cement Chemistry, p. 357-359, Thomas Telford, London, 1997.

Verbeck, G.J., 1958. "Carbonation of Hydrated Portland Cement," PCA Research Department Bulletin, **87**, 1958.

4.4 Sulfate Attack

Sulfate attack represents a complex set of chemical and physical processes and can not be characterized by a single mechanism. Hydrated and unreacted phases in portland cement based materials react with sulfate ions to form solid phases. Microstructural changes and mechanical strains are associated with these reactions that can lead to degradation by strength loss (loss of cementitious properties), spalling, and/or cracking [Ferraris, 1997]. See Figure 4-6.

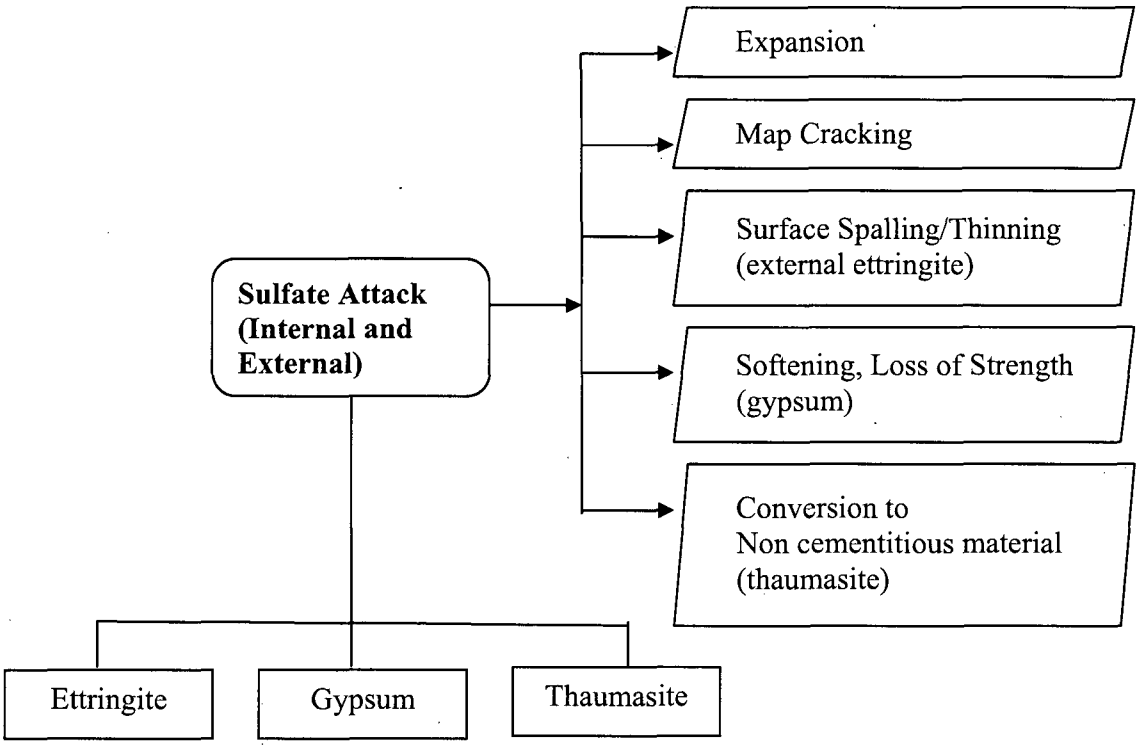

Figure 4-5. Sulfate attack processes and consequences.

Sulfate attack is typically managed by minimizing the reactive component (tricalcium aluminate) in the cement. The American Concrete Institute (ACI) classifies sulfate exposure into four degrees of severity depending on the sulfate concentrations in soil and water in contact with concrete. See Table 4-1.

Table 4-1. ACI Sulfate Resistance Table [ACI 201.2R, 2005].

Relative degree of sulfate attack	Percent water soluble sulfate (as SO_4^{2-}) in the soil samples	Sulfate (as SO_4^{2-}) in the water samples (mg/L)
Negligible	0.00 to 0.10	0 to150
Positive	0.10 to 0.20	150 to 1,500
Severe	0.20 to 2.00	1,500 to10,000
Very Severe	2.00 or more	10,000 or more

4.4.1 Description and Mechanism

The source of the deleterious sulfate can come from the environment (external) or from the cement/concrete itself (internal). Internal and external sulfate attack in concrete involves formation of sulfate-bearing phases (ettringite, gypsum, or thaumasite) in addition to altering the microstructure and composition of the C-S-H phase (sulfate attack decalcification). These changes can lead to local expansion and the development of crack networks which increase the total porosity and permeability of the material [Diamond and Lee, 1999].

External Sulfate Attack. External sulfate attack is typically the result of exposure to sodium sulfate solutions, magnesium sulfate solutions (sea water and arid conditions), or calcium sulfate (gypsum or anhydrated contaminated aggregate). This discussion is limited to exposure to sodium sulfate solutions and to portland cement in general.[16] The chemical reactions between sulfate resistant portland cements and sodium sulfate are similar to those for ordinary portland cements except that the extent of decalcification of C-S-H binder phase and cracking are greatly reduced.

External sulfate attack proceeds from the surface exposed to the sulfate-rich environment by inward advancement of a series of reaction fronts. External sulfate attack is typically manifested by replacement of monosulfate (AFm)[17] by ettringite (via dissolution and precipitation) at the reaction front plus depletion of calcium hydroxide at the surface. Gypsum is also typically precipitated at the exposed surface. Formation of ettringite from monosulfate (Equation 4) requires Ca^{2+}, SO_4^{2-} and H_2O. It also requires availability of $Al(OH)_4^-$ ions. Sulfate is provided by the external environment; calcium ions are initially provided by calcium hydroxide in the matrix; and aluminate ions are provided by monoslfate or unreacted C_3A. C-S-H, hydrotalcite or hydrogarnet phases are not sources of readily available aluminate.[18]

Equation 4 $C_4A\bar{S}H_{12} + 2Ca^{2+} + 2SO_4^{2-} + 20H_2O \longrightarrow C_6A\bar{S}_3H_{32}$

After the $Ca(OH)_2$ has been consumed or is less readily available, calcium is leached from the C-S-H binder phase with the result that the Ca/Si ratio of this phase decreases. As exposure to sulfate ions progresses, gypsum, $CaSO_4 \cdot 2H_2O$, is also formed which consumes more Ca^{2+} ions and continues to drive decalcification of the solid phases in the system.[19]

---

[16] Exposure to $MgSO_4$ solutions is more aggressive than exposure to Na_2SO_4 solutions and calcium sulfate and is typically associated with internal sulfate attack when gypsum is present in aggregates. Since Mg concentration in SRS groundwater is very low (< 0.5 mg/L) magnesium attack was not considered in this analysis of degradation mechanisms.

[17] AFm phases have the general formula $[Ca_2(Al, Fe)(OH)_6] \cdot xH_2O$ where X denotes one formula unit of a singly charged anion or half a formula unit of a doubly charged anion. The m refers to mono and refers to a single formula unit of CaX_2 in another way of writing the formula, i.e., $C_3(A,F) \cdot CaX_2 \cdot yH_2O$ where $y = 2(x+3)$.

[18] Cement notation is used to represent oxides in chemical formulas and equations. $A = Al_2O_3$, $C = CaO$, $F = Fe_2O_3$, $H = H_2O$, $K = K_2O$, $M = MgO$, $N = Na_2O$, $P = PO_4$, $S = SiO_2$, $\bar{S} = SO_4$. Ionic species, such as, Ca^{2+} ions, contribute one Ca atom to the formula. Sulfate ion, SO_4^{2-}, contributes one S atom ($\bar{S}$) to the formula.

[19] Gypsum formation takes place by reaction between calcium hydroxide or calcium ions, sulfate ions and water. Gypsum formation in itself typically leads to weakening or softening and contributes to the overall degradation associated with sulfate attack.

External sulfate attack involves substantial microstructural changes and an increase in permeability as the result of the dissolution of calcium hydroxide, decalcification of calcium silicate hydrates and formation of new sulfate phases [Allan 1997]. Although expansion has been widely attributed to ettringite formation alone, decalcification, dehydration, and subsequent rehydration of the C-S-H gel, may actually be responsible for much of the observed strength loss, micro cracking and overall structural damage [Taylor 1997(a)]. Expression of external sulfate attack on the macro-scale is represented by extensive interconnected network of cracks on the exposed surface which lead to spalling and a progressive reduction in thickness of sound material. In reinforced concrete, reduction in thickness of the cover over the rebar contributes to steel corrosion, decrease in tensile strength, and a reduction of service life.

Internal Sulfate Attack. Internal sulfate attack (represented by either delayed ettringite formation (DEF) or heat-induced internal sulfate attack) refers to the situation where the source of sulfate is internal to concrete. Causes of delayed ettringite formation are discussed elsewhere [Thaulow, 1997, Thomas, 2001]. Reviews of internal sulfate attack are provided elsewhere [ASTM 1997 and Taylor, 1997(b)]. The expression of internal sulfate attack is severe cracking and the formation of a crack network throughout the entire cementitious element.

A special case of internal sulfate attack applies to cement stabilized waste forms which contain high concentrations of sulfate. A sodium substituted AFm phase, referred to as U-Phase has been detected in waste forms with high sulfate contents. This phase has been shown to be responsible for degradation of simulated samples [Li, 1997]. U Phase has the potential to induce deterioration in waste forms through two mechanisms; expansion and transformation to ettringite [Moranville and Li, 1999]. U-Phase is unstable below a pH of about 12.5 and transforms to ettringite as the result of leaching. The consequence of this transformation on the microstructure is severe cracking [Li, 1997].[20]

In the case of tank closure, sulfate ions are present in the waste residuals that may be left in the tanks.[21] The mineralogy of tank residual-cement grout mixtures has not been characterized and crack formation as the result of internal sulfate attack has not been investigated for tank grout aging scenarios.

Sulfate Carbonate Attack. Thaumasite, a hydrated calcium silicate sulfate-carbonate solid solution, can form through a combination of sulfate attack and carbonation. Conditions

---

[20] Sulfate phases and sulfate–carbonate solid solution phases have been detected in SRS saltstone which is formed in a similar chemical system as the result of mixing tank supernate with a blend of cement, slag and fly ash to produce a waste form. A phase similar to the U-Phase, a Na_2O substituted hexagonal AFm phase, and gypsum have been detected in cured saltstone.

[21] Sulfate ions can also originate from the cement, the supplementary cementing materials, the chemical admixtures, the aggregates (such as pyrite inclusions in coarse aggregates), or a combination of the above.

required for thaumasite formation are presented elsewhere [Crammond, 1997]. Two mechanisms have been proposed for its formation:

- Thaumasite may form from ettringite by substitution of Al^{3+} by Si^{4+} in the presence of CO_3^{2-}, or
- Thaumasite may form as the result of the direct interaction among C-S-H, sulfate ions and carbonate ions.

Thaumasite is stable at temperatures below about 10°C (50°F) and is responsible for severe damage to concrete structures by destroying the binding capacity of the C-S-H in the cement matrix. Because the attack is on the silicate and not the aluminate constituents in the hydrated cement, sulfate-resistant portland cement does not extend the service life.

Expression of thaumasite formation is complete loss of integrity and is described as going from concrete to "mush." This mechanism of degradation is mentioned because carbonate and sulfate phases are present in the residual waste that may be left in the tank and the temperature in the buried setting will be near the upper stability limit for the pure phase. However, because data are not available on the interaction between the waste constituents and cementitious grouts, this mechanism will not be considered in this analysis.

4.4.2 Models for Sulfate Attack [Glasser, 2007]

Many factors influence the degradation of concrete by sulfate attack. The pore structure of the material, which is a non-linear consequence of the water to cementitious binder ratio, and the type of binder (portland cement, blended cements, etc.) are very important parameters in determining the rate of sulfate penetration and the consequences (expansion) of sulfate attack [ACI 201.2R, 2005; Hearn and Young, 1999; Khatri and Sirivavatnanon,1997; Ouyang, et. al, 1988].

Empirical, mechanistic, and numerical models have been proposed for predicting the behavior of cementitious materials exposed to sulfate ions. The empirical models estimate the sulfate resistance factor, the expansion due to sulfate attack reactions, or the depth of visible degradation [Glasser, 2007]. Mechanistic models typically attempt to take into account the mechanisms leading to the deterioration and usually predict the rate of sulfate attack and fractional or volumetric expansion. These types of models have limited predictive capabilities [Glasser, 2007]. They tend to overestimate the rate of degradation for low to mild conditions.

Ionic transport models simulate the chemical reactions occurring during sulfate attack. They rely on dissolution-precipitation reactions coupled to descriptions of ion transport through the cementitious matrix (estimated by diffusion). In some cases they also estimate the damage caused by expansion [Glasser, 2007, Marchand, 1999 and 2002]. These more sophisticated models require well characterized concrete specimens and knowledge of the pore solution chemistry and phase mineralogy.

INEEL Tank Closure PA Approach. In the INEEL PA, a simple empirical model developed by Atkinson and Hearne, 1984, was used to estimate coupled external sulfate attack and

magnesium attack (formation of $Mg(OH)_2$, another expansive phase) [INEEL PA Appendix E, 2003]. This model is based on the observed loss of cement at block corners after 5 years in 0.19 M Na_2SO_4 solution. The depth of attack on the block was 42 mm and indicated a linear relationship with time. The rate of attack was assumed to be proportional to sulfate concentration in the solution and tricalcium aluminate content in the cement. They also evaluated $MgSO_4$ attack because the local soil contains magnesium. The depth of attack in $MgSO_4$ solution was approximately twice that of the Na_2SO_4 solution. Using these assumptions, the depth of concrete degradation from sulfate and magnesium attack was estimated by the following equation:

Equation 5 $x = 0.55\ C_{C3A}\ (Mg^{+2} + SO_4^{-2})\ t$

where:

x = depth of concrete degradation (cm)

C_{C3A}= weight percent of tricalcium aluminate in the unhydrated cement [22]

Mg^{+2}, SO_4^{-2} = concentrations of these ions in bulk solution (moles/L)

t = time (years)

Internal sulfate attack is acknowledged as a potential degradation mechanism for concrete in contact with the tank waste because the residual waste left in the tank may contain sulfate. At this time, the residual has not been characterized sufficiently with respect to mineralogy, chemistry, and interactions with the cementitious grout that will be used to fill the tanks to perform an evaluation of the impact on the grout durability.

4.4.3 References for Sulfate Attack

Allan, M.L. and L.E. Kukacka, 1997. "Permeability and Leach Resistance of Grout-Based Materials Exposed to Sulphates," p. 436-443, Proceedings of the Materials research Society's Symposium on Mechanisms of Chemical Degradation of Cement-Based Systems, Boston, November 27-30, 1995, Published in Mechanisms of Chemical Degradation of Cement-Based Systems, K. L. Scrivener and J.F. Young, Eds.,E&FN SPON, London, 1997.

American Concrete Institute, 2005. Guide to Durable Concrete, ACI 202.2R-05, ACI Manual of Concrete Practice Part1, Materials and General Properties of Concrete, ACI , Farmington Hills, MI, 2005.

American Society of Testing and Materials, 1997. "ASTM Symposium on Internal Sulfate Attack," R.D. Hooton and R.L. Roberts, chairmen, published in Cement and Concrete Aggregate, **21**, 1999.

---

[22] Cement notation is used to represent oxides in chemical formulas and equations. A = Al_2O_3, C = CaO, F = Fe_2O_3, H = H_2O, K = K_2O, M = MgO, N = Na_2O, P = PO_4, S = SiO_2, $\bar{S}$ = SO_4.

Atkinson, A, and H. A. Hearne, 1984. "An Assessment of the Long-Term Durability of Concrete in Radioactive Waste Repositories," AERE-R11456, Harwell, U.K., 1984 summarized in Walton, J.C., L.E. Plansky and R.W. Smith, 1990 (see reference below).

Crammond, N.J. and M.A. Halliwell, 1997. "Assessment of the Conditions Required for the Thaumasite Form of Sulphate Attack," p.185-192, Proceedings of the Materials research Society's Symposium on Mechanisms of Chemical Degradation of Cement-Based Systems, Boston, November 27-30, 1995, Published in Mechanisms of Chemical Degradation of Cement-Based Systems, Eds., K. L. Scrivener and J.F. Young, E&FN SPON, London, 1997.

Diamond, S. and R. J. Lee, 1999. "Microstructural Alterations Associated with Sulfate Attack in Permeable Concretes," p.123-173, Materials Science of Concrete Sulfate Attack Mechanisms, J. Marchand and J. P. Skalny Eds., American Ceramic Society, Westerville, OH, 1999.

Ferraris, C.F., J. R. Clifton, P.E. Stutzman, and E.J. Garboczi, 1997. "Mechanisms of Degradation of Portland Cement-Based Systems by Sulfate Attack," p.185-192, Proceedings of the Materials research Society's Symposium on Mechanisms of Chemical Degradation of Cement-Based Systems, Boston, November 27-30, 1995, Published in Mechanisms of Chemical Degradation of Cement-Based Systems, Eds., K. L. Scrivener and J.F. Young, E&FN SPON, London, 1997.

Glasser, F.P., 1999. "Reactions Between Cement Paste Components and Sulfate Ions," p. 99-122, Materials Science of Concrete Sulfate Attack Mechanisms, J. Marchand and J. P. Skalny eds., American Ceramic Society, Westerville, OH, 1999.

Glasser, F. P., J. Marchand and E. Samson, 2007. "Durability of Concrete – Degradation Phenomena Involving Detrimental Chemical Reactions, Key note address, 2007.

Hearn, N., and F. Young, "W/C Ratio, Porosity and Sulfate Attack – A Review," p.189-205, Materials Science of Concrete Sulfate Atach Mechanisms, J. Marchand and J. P. Skalny eds., American Ceramic Society, Westerville, OH, 1999.

Hooton, R. D., 2006. "A Review of Different Forms of Sulfate Attack," Cementitious Materials for Waste Treatment, Disposal, Remediation, and Decommissioning Workshop, December 12-14, 2006, Savannah River National Laboratory, Aiken SC, 2006.

INEEL PA Appendix E, 2003. "Degradation Analysis of the Grouted Tank/Vault and Piping System at the Idaho Nuclear Technology and Engineering Center Tank Farm Facility and Preliminary Results for the Detailed Analysis of Releases from the Grouted Pipe and Encasement System, Revision 1,"p. E13, E21, INEEL, Idaho Falls, ID, 2003.

Khatri, R. P., V. Sirivivatnanon, and J. L. Yang, "Role of Permeability in Sulfate Attack," *Cement and Concrete Research*, **27**[8], p.1179-1189, 1997.

Li, G. and P. Le Bescop, 1997. "Degradation Mechanisms of Cement-Stabilized Wastes by Internal Sulfate Associated with the Formation of the U Phase," p. 427-435, Proceedings of the Materials research Society's Symposium on Mechanisms of Chemical Degradation of Cement-Based Systems, Boston, November 27-30, 1995, Published in Mechanisms of Chemical Degradation of Cement-Based Systems, Eds., K. L. Scrivener and J.F. Young, E&FN SPON, London, 1997.

Marchand, J., E. Samson, Y. Maltais, and J. J. Beaudoin, 2002. "Theoretical Analysis of the Effect of Weak Sodium Sulfate Solutions on the Durability of Concrete," *Cement and Concrete Composites*, **24**[3/4], p.317-329, 2002.

Marchand, J., E. Samson, and Y. Maltais, 1999. "Modeling Microstructural Alterations of Concrete Subjected to External Sulfate Attack," p. 211-257. Materials Science of Concrete Sulfate Atach Mechanisms, J. Marchand and J. P. Skalny Eds., American Ceramic Society, Westerville, OH, 1999.

Moranville, M. and G. Li, 1999. "The U-Phase – Formation and Stability," p. 175-188, Materials Science of Concrete Sulfate Attack Mechanisms, J. Marchand and J. P. Skalny Eds., American Ceramic Society, Westerville, OH, 1999.

Ouyang, C., A. Nanni, and W. F. Chang, 1988. "Internal and External Sources of Sulfate Ions in Portland Cement Mortar: Two Types of Chemical Attach," *Cement and Concrete Research*, **18**[5], p.699-709, 1988.

Skalny, J. and J. S. Pierce, 1999. "Sulfate Attack Issues: An Overview," p. 49 to 63, Materials Science of Concrete Sulfate Attach Mechanisms, J. Marchand and J. P. Skalny Eds., American Ceramic Society, Westerville, OH, 1999.

Taylor, J.F.W., 1997(a). Cement Chemistry, p. 368-378, Thomas Telford, London, 1997.

Taylor, J.F.W., 1997(b). Cement Chemistry, p. 374-378, Thomas Telford, London, 1997.

Thaulow, N., V. Johansen, and U.H. Jakobsen, 1997. "What Causes Delayed Ettringite Formation?," p.219-226, Proceedings of the Materials research Society's Symposium on Mechanisms of Chemical Degradation of Cement-Based Systems, Boston, November 27-30, 1995, Published in Mechanisms of Chemical Degradation of Cement-Based Systems, Eds., K. L. Scrivener and J.F. Young, E&FN SPON, London, 1997.

Thomas, M. 2001. Delayed Ettringite Formation in Concrete: Recent developments and Future Directions," p.435-481, Materials Science of Concrete VI, Ed. S. Mindess and J. Skalny, American Ceramic Society, Westerville, OH, 43081.

Walton, J.C., L.E. Plansky and R.W. Smith, 1990. "Models for Estimation of Service Life of Concrete Barriers in Low-Level Radioactive Waste Disposal," NUREG/CR—5542, TI91 000576, EG&G Idaho, Inc., Idaho Falls, ID 83415.

4.5 Alkali Aggregate Reactions

4.5.1 Description and Mechanism

Alkali-aggregate reactions (AAR) take place in concrete when alkalis in the pore solution or from an alkali-rich external source react with dolomite (alkali-carbonate reaction) or certain types of siliceous aggregate (alkali-silica reaction) to form hygroscopic gels which can imbibe water and expand. Expansion causes internal stresses that result in disruption of the microstructure and cracking. Measurements of the stresses associated with alkali-silica reactions indicate a strong influence of creep on the mechanical response of the material undergoing this type of expansion [Ferraris, 1997].

The necessary conditions for AAR are a sufficiently high alkali content in the cement or environment, and reactive aggregates. The process and mechanism of alkali-silica reaction, however, remains a subject of considerable debate among the scientific community, despite the numerous research projects carried out on that topic [Helmuth, 1992, Helmuth, 1993].

The alkali-silica gel often appears in pop-outs or exudes from cracks on unrestrained concrete surfaces. The crack network consists of fine cracks and larger "map cracks". If the source of the alkali is internal to the concrete element, the crack network is formed throughout the entire cementitious element. In reinforced concrete, the cracks tend to form parallel to the reinforcement. A characteristic of alkali aggregate reaction is that cracks often pass through the aggregate. See Figure 4-6.

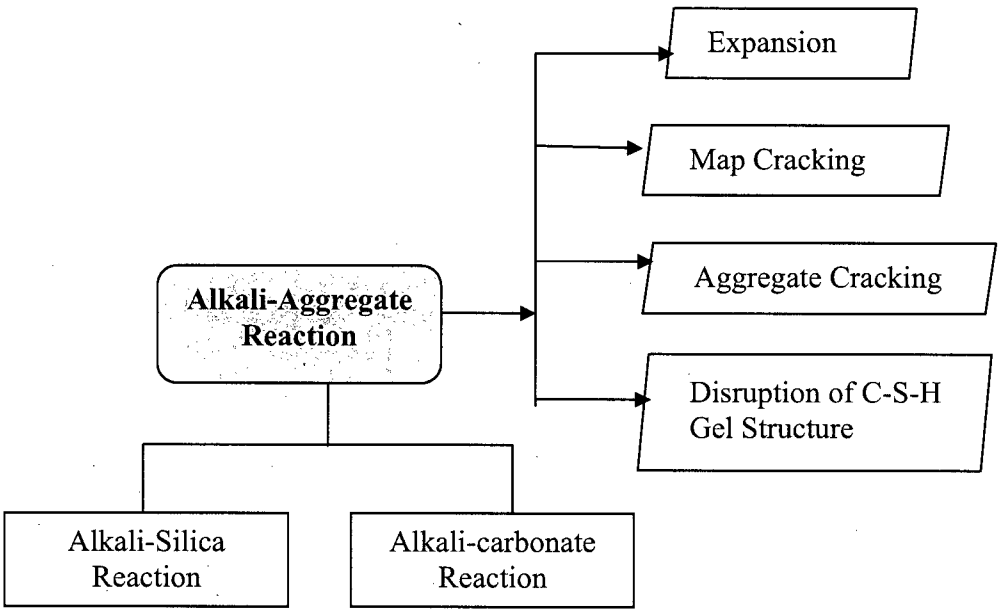

Figure 4-6. Alkali-Aggregate processes and consequences.

4.5.2 Models for Alkali-Aggregate Reactions

Results of numerous studies on AAR in concrete and mortars have been published [Diamond, 1976, Dent Glasser, 1982, Pettifer, 1980, Strubble, 1982]. Mechanistic and applied engineering summaries of this form or degradation are presented elsewhere [Taylor, 1999]. Due to the complex nature of this mechanism and the unique properties of susceptible aggregates, this form of degradation has not been modeled. Instead, emphasis has been placed on developing testing to identify susceptible aggregates, and to develop specifications to limit the amount of alkali in the cement [Stark, 1993, Dobrowolski, 1998].

The concentrations of alkalis in the SRS soils are very low and highly reactive aggregates are not used in SRS cementitious materials. However, the residual waste that may be left in the HLW tanks is high in alkalis. These residuals will be in contact with (covered) or mixed with cementitious fill material. The alkalis in the residual heel may also be susceptible to leaching over long times depending on the aging of the entire tank system and may thereby contact the concrete base mat underlying the tanks. The consequences of these changes depend on aging of the base mat and tank and were not analyzed here. At this time, data on the interactions between the residual waste and the tank fill grout are not available. Consequently, no further analysis can be performed on this unique situation.

INEEL Tank Closure PA Approach. This mechanism was described but not analyzed in the INEEL Tank Closure PA [INEEL Appendix E, 2003].

4.5.3 References Alkali-Aggregate Reactions

Constantiner, D. and S. Diamond, 1997. "Fixation of Alkalis in Cement Pore Solutions," p.67-74, Proceedings of the Materials research Society's Symposium on Mechanisms of Chemical Degradation of Cement-Based Systems, Boston, November 27-30, 1995, Published in Mechanisms of Chemical Degradation of Cement-Based Systems, Eds., K. L. Scrivener and J.F. Young, E&FN SPON, London, 1997.

Daimond, S. 1976. "A Review of Alkali-Silica Reaction and Expansion Mechanisms 2. Reactive Aggregates," *Cement and Concrete Research*, **6**[4], p.549-560, 1976.

Dent Glasser, L. S. and N. Kataoka, 1982. "On the Role of Calcium in the Alkali-Aggregate Reaction," *Cement and Concrete Research*, **12**[2], p. 321-331, 1982.

Dobrowolski, J. A., 1998. Concrete Construction Handbook, 4th Ed., p. 7.15-7.19, McGraw Hill, NY.

Ferraris, C.F., J. R. Clifton, E. J. Garboczi, and F. L. Davis, "Stress Due to Alkali-Silica Reactions in Mortars," p.75-82, Proceedings of the Materials research Society's Symposium on Mechanisms of Chemical Degradation of Cement-Based Systems, Boston, November 27-30, 1995, Published in Mechanisms of Chemical Degradation of Cement-Based Systems, Eds., K. L. Scrivener and J.F. Young, E&FN SPON, London, 1997.

Helmuth, R. and D. Stark, 1992. "Alkali-Silica Reactivity Mechanisms," Material Science of Concrete III, Ed. J. Skalny, American Ceramic Society, Westerville, OH, 1992.

Helmuth, R., 1993. "Alkali Silica Reactivity: "An Overview of Research," SHRP Report C-342, National Research Council, Washington DC, 1993.

INEEL PA Appendix E, 2003. "Degradation Analysis of the Grouted Tank/vault and Piping System at the Idaho Nuclear Technology and Engineering Center Tank Farm Facility and Preliminary Results for the Detailed Analysis of Releases from the Grouted Pipe and Encasement System, Revision 1,"p. E16, E20, INEEL, Idaho Falls, ID, 2003.

Pettifer, K. and P. J. Nixon, 1980. "Alkali Metal Sulphate — a Factor Common to Both Alkali Aggregate Reaction and Sulphate Attack on Concrete," *Cement and Concrete Research*, **10**[2], p.173-181, 1980.

Stark, D., B. Morgan, B., P. Okamoto, 1993. "Eliminating or Minimizing Alkali-Silica Reactivity," SHRP-C343, National Research Council, Washington, DC, 1993.

Struble, L. J. and S. Diamond, 1982. *J. Am. Ceramic Society* [64], p. 652.

Taylor, H. F. W., 1997(c). Cement Chemistry, p. 361-368, Thomas Telford, London, 1997.

4.6 Reinforcing Steel Corrosion

4.6.1 Description and Mechanisms

Corrosion of steel reinforcement is the most common cause of concrete deterioration. Metal rebar oxidation in the presence of water results in the formation of iron hydroxide, rust. Progressive oxidation of steel rebars results in volumetric expansion as corrosion products are formed.[23] This expansion causes de-bonding between the concrete and steel and is responsible for micro cracking and a loss in tensile strength of the structural element. As the process progresses, continued expansion results in more cracking and spalling of the concrete cover which exposes more steel rebar and accelerates corrosion and loss of mechanical properties. The ultimate expression of rebar corrosion is structural collapse due to loss of material and/or mechanical loading. See Figure 4-7.

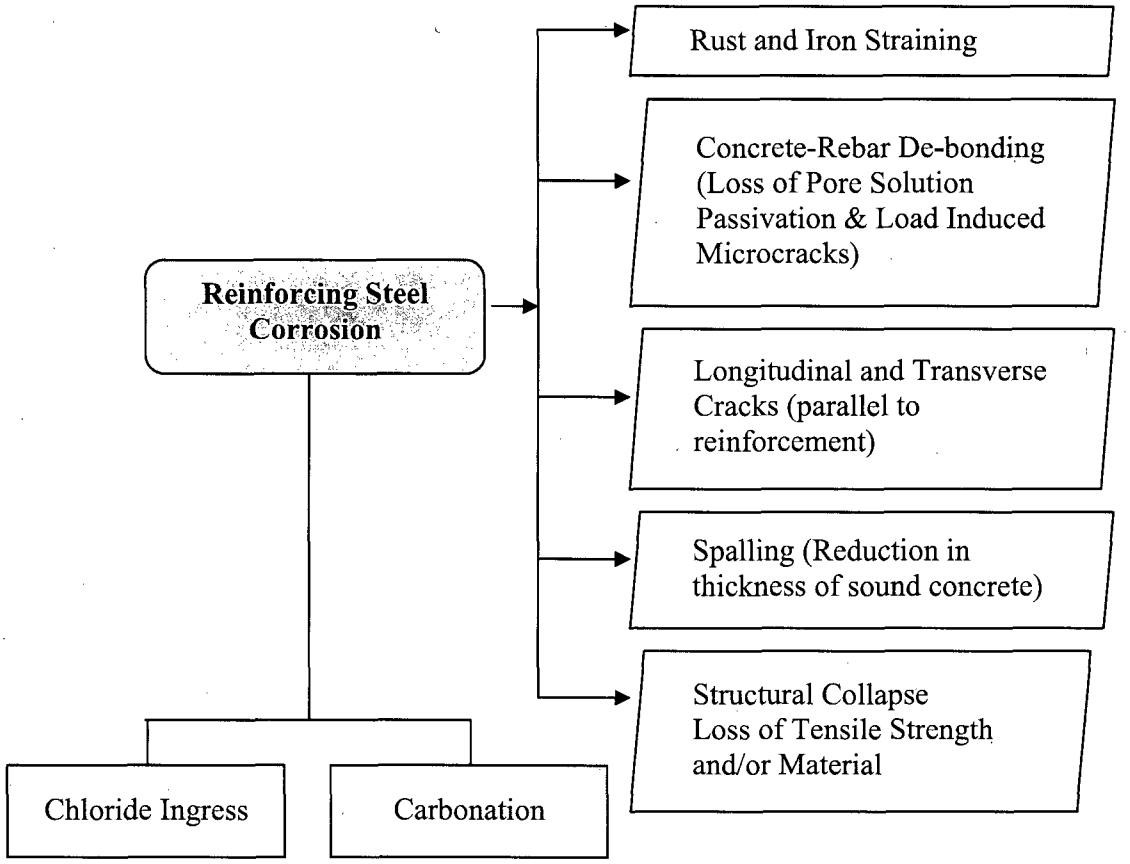

Figure 4-7. Rebar corrosion processes and consequences.

[23] The microstructure development of the corrosion layers on steel in reinforced concrete and the behavior of steel in simulated concrete pore solutions have been studied and reported elsewhere [Constantinou, 1997 and Wheat, 1997, respectively]. The effect of existing cracks on rebar corrosion and the effects of rebar corrosion induced cracks on subsequent rebar corrosion are discussed elsewhere [Hearn and Figg, 2001].

In general, the processes responsible for rebar corrosion are confined to the transport properties of the cement paste. The aggregates are not involved in the rebar corrosion process. The presence and transport of water, oxygen, and ionic species, the corrosion products themselves, and current necessary to support corrosion are responsible for the degradation [Rosenberg, 1989]. With respect to reinforcement corrosion, the controlling parameters are: 1) the composition and quantity of the pore solution, 2) the pore structure of the cement paste, and 3) the presence of $Ca(OH)_2$ in the hardened paste.

In sound reinforced concrete, the steel reinforcing bars are passivated by the alkaline chemistry (pH ~ 12.5) of the pore solution. Passivation occurs when the corrosion product is insoluble. The result is the formation of a thin protective film on the steel surfaces.[24] For steel in concrete, the alkaline nature of the pore solution and the availability of oxygen in the system, produce a stable oxide film on the metal surface. Under these ideal conditions, the corrosion rate is not zero but rather it is very slow and equivalent to dissolution or oxidation of about 0.1 μm / year from the steel surface [Hansson, 1984, Rosenberg, 1989].

Once general or local de-passivation occurs, corrosion is initiated. The rate is a function of the availability of oxygen, water, and chemical corrodents such as chloride ions. The stability of the film is also a function of temperature, relative humidity, degree of saturation, tensile stress.[25]

The pore solution chemistry determines whether the embedded steel will be passivated or whether it will actively corrode. The pore structure of the paste especially the connectivity of the pores will determine the availability of oxygen and moisture (both of which are necessary to maintain passivation) at the steel surface. The pore structure also determines the rate of penetration of corrodents such as chlorides and of CO_2. The $Ca(OH)_2$ buffers the pH of the pore solution even though it has limited solubility in the pore solution and most of it is embedded in the cement paste. The higher the calcium hydroxide concentration, the longer it takes a carbonation front to penetrate the concrete cover to the steel surface. Calcium hydroxide is reported to provide another benefit in that it is precipitated as a protective coating (consisting of hexagonal platelets) on the steel surfaces and pore walls [Rosenberg, 1989, Page, 1982].

Corrosion of steel in concrete occurs by electrochemical reactions. The maintenance of passivity in steel embedded in concrete requires high pH and the presence of both water and oxygen. A reduction in pH brought about by carbonation will lead to active corrosion. The absence of water will be a cessation of the corrosion process. In the absence of oxygen and

---

[24] Ions in the pore solution, such as NO_2^-, can inhibit rebar corrosion.

[25] Corrosion may be inhibited if the oxygen concentration is low enough and will not necessarily occur even if the concrete in contact with the steel is completely carbonated. However, maintenance of the passive film requires some oxygen and if the supply of oxygen is very restricted, as in the case of concrete buried under moist ground, all of the oxygen can be used up. In theory, corrosion can occur through reduction of water to hydrogen but in practice, corrosion rates under these conditions are similar to those when a passive film exists [Hansson, C. M. 1984]. (The effect of radiolysis and generation of hydrogen through radiolysis of water on the corrosion of metal rebar in concrete is beyond the scope of this review.)

given a pH of >9, the corrosion process will continue but with the evolution of hydrogen gas at the cathode. This reaction has a higher rate than the case with oxygen but it is still very slow.

For steel in concrete, the iron is oxidized at the anode. The electrons released at the anode flow through the steel to the cathode where they are consumed by the cathodic half-cell reaction.

Anode Reaction: $Fe \longrightarrow Fe2^{+} + 2e^{-}$

Cathode Reaction: $2H_2O + O_2 + 4e^{-} \longrightarrow 4OH^{-}$
For alkaline pores solution and access to air (oxygen)

Cathode Reaction: $2H_2O + 2e^{-} \longrightarrow H_2 + 2OH^{-}$
For pores solution with pH < 9 and no access to oxygen (reducing)

The two primary causes of the breakdown of the passivation layer on steel embedded in concrete are:

1. The presence of chloride ions either in the concrete raw materials or from an external source such as sea water or deicing salts, and
2. A decrease in the pH of the concrete pore solution because of reaction of the cement paste with atmospheric or dissolved CO_2 (carbonation).

The morphology of the corrosion process depends on the distribution of the anodes and cathodes and their relative areas. If the anodes and cathodes are irregularly distributed and change position during the corrosion process, the attack will be more or less uniform. If the anodes are located at fixed points and the anode/cathode area ratio is small, localized attack will develop.

Chloride Ingress. The concrete degradation mechanism which results in corrosion of reinforcing steel due to ingress of chloride ions is referred to as chloride- induced corrosion. This process has been well documented especially with respect to marine structures and exposure to deicing salts [Rosenberg, 1989, Thomas, 2001, Hope, 1985, Page, 1986, Roy, 1986].[26]

Even in high pH environments (pore solution), chloride ions cause localized destabilization of the passivating oxide film on steel rebar. The most rapid form a Cl- penetration occurs by capillary suction into more or less dry concrete and is typically encountered in structures in the region of the water-air interface. In saturated conditions, the penetration rate is controlled by diffusion of the chloride ion in the pore solution and is slower. Additional factors that control the rate of chloride corrosion include:

---

[26] Exposure of un-reinforced cement-based materials to chloride ions does not result in deterioration of hydraulic or mechanical properties [Glasser, et al., 2007]. For un-reinforced concrete, chemical reactions between Cl^{-} ions and hydrated cement phases result in chloride binding and include formation of Friedel's salt, $3CaO{\cdot}Al_2O_3{\cdot}CaC_{l2}{\cdot}10H_2O$, or Kuzel's salt, $3CaO{\cdot}Al_2O_3{\cdot}1/2CaC_{l2}{\cdot}1/2CaSO_4{\cdot}10H_2O$, solid solution phases, which do not disrupt the microstructure.

- The $[Cl^-]$ / $[OH^-]$ ratio in the pore solution.
- Transport through micro cracks.
- Chloride binding capacity of the matrix work together to determine the chloride ingress. For example, C-S-H gel and calcium aluminate can react with chloride ions for form Friedel's salt.

The mechanism for chloride de-passivation involves incorporation of the chloride ions in the film structure by replacing some of the oxygen. This increases the conductivity and solubility of the film and creates galvanic cells that drive dissolution of the iron. This process is described elsewhere [Rosenberg, 1989]. The dissolved iron precipitates as oxides that are progressively oxidized and hydrated and are responsible for stresses that lead to cracking. The increase in molecular volume of the oxides and hydrated oxides relative to the original metal can result in a volume increase of up to six times as illustrated in Figure 4-8. For concrete that is saturated, the dissolved iron can diffuse through the pores and cracks to the external surface and cause rust stains without cracking.[27]

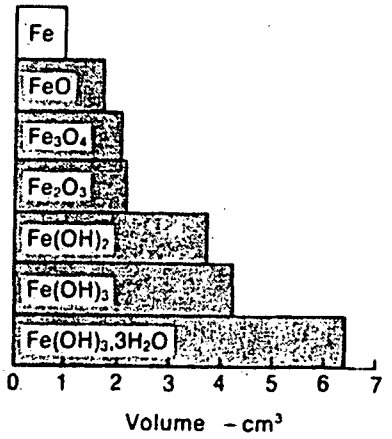

Figure 4-8. Relative molar volume increase associated with iron oxidation [Rosenberg, 1989, after A. Nielsen, 1985].

Carbonate Induced De-Passivation. The carbonation process was described in an earlier section. When the carbonation front reaches the steel reinforcement, the passive film is no longer stable due to the decrease in alkalinity and active corrosion is initiated. General corrosion of the steel is typical because the carbonation front penetrates more or less uniformly through the cover to the steel. In addition to the availability of CO_2, moisture in the pores must also be present for corrosion to occur at a significant rate. Wet-dry cycling is the most aggressive environment for rebar corrosion. In a dry environment (low humidity), gases penetrate easily through empty pores but the lack of water in the pore will inhibit both carbonation and formation of corrosion products. Saturated conditions are also not the most

[27] Iron staining on exposed surfaces is a simple and useful indicator of rebar corrosion initiation. This is illustrated in many structures including the Z-Area waste disposal vaults.

aggressive because the advancement of the carbonation front is controlled by diffusion of dissolved carbonate species through the pore solution.

4.6.2 Models for Chloride Induced Corrosion

Early models were based on diffusion of chloride as a function of time which evolved to include empirical relationships that attempted to account for bound chloride. Empirical models for chloride induced corrosion of metal developed by Clear (1976) Bazant (1979a and b), and Subramanian and Wheat (1988) are summarized by Walton, et al., 1990.

The current trend in modeling focuses on multi ion transport approaches. Samson and Marchand developed a model in which chloride transport is based on mass and energy conservation plus chemical interactions between chlorides and relevant phases in the hydrated cement (ionic exchange) [Samson, 2007].

In the Samson model, steel corrosion is initiated when the chloride concentration in the pore solution in contact with the steel reaches a threshold value.[28] A comprehensive review of threshold values is presented elsewhere [Alonso 2000]. A threshold value of 0.3% total chloride per weight of cement (approximately 0.5g of total chloride per kg of concrete) is accepted as standard practice for most engineering analyses of concrete degradation [US Federal Highway Administration, 1998].

The time needed to reach the critical chloride content for corrosion of reinforcing steel is referred to as the initiation period [Tuutti, 1982]. It is a function of several parameters including, properties (porosity, permeability, saturation, thickness, etc.) of the concrete covering the rebar and the exposure conditions. Modeling penetration of chlorides into cement-based materials (accounting for transport and chemical reactions) provides part of the information required to predict the time length of the initiation period by providing the time evolution of the total chloride content as a function of location in the concrete element. This information needs to be combined with an appropriate threshold concentration to predict the corrosion initiation time. The current predictive modeling assumes cracking and crack propagation occurs when the threshold chloride concentration at the rebar is reached.

4.6.3 Models for Carbonation-Induced Corrosion.

Numerous diffusion-based models for coupled transport of moisture, carbon dioxide, and calcium have been developed to predict of the depth of carbonation in cementitious materials [Bary, 2004, Saetta, 1993, and 2004, Song, 2006]. These models were reviewed by Glasser, et al. who identified the main shortcomings as:

1) The prediction of the pH drop is not part of the model because OH- concentration is neglected.
2) Na and K ions in the pore solution are involved in the carbonation process but not in the coupled transport.
3) Coupling chloride ingress (including incorporation Friedel's salt and subsequent release of chloride upon carbonation) and carbonation are not included

[28] The threshold value is also dependent on the hydroxyl ion concentration and is often expressed as [Cl]/[OH] or by the total amount of chloride in the material (wt. %).

These models predict the depth of carbonation and assume rebar corrosion results in degradation of the reinforced concrete structure (cracking and strength loss) when the depth of carbonation equals the thickness of the rebar cover.

INEEL Tank Closure PA Approach. INEEL used a simple shrinking core model to estimate the depth of carbonation as a function of time [INEEL PA Appendix E, 2003]. This approach is based on gaseous diffusion which is conservative and is described in Equations 6 to 8. The degree of saturation of the concrete is important in carbonation models because the carbonation rate increases as the saturation decreases (fraction of pore volume occupies by air increases). The carbonation rate is greatest at about 50 % relative humidity [Verbeck, 1958]. The diffusion of gaseous CO_2 is approximately four orders of magnitude greater that aqueous diffusion.

INEEL assumed air phase diffusion to be the dominate mechanism for CO_2 transport into concrete. See Equation 6.

Equation 6. $$X_0 = \left(2D\tau_{\text{air}}\Phi_{air}\frac{(C_{atm})t}{C_s} \right)^{1/2}$$

The leaching process is assumed to be controlled by diffusion and can be described as a molar out flux of Ca. The flux is described in Equation 7.

Equation 7. $$N = -D\tau_{\text{air}}\Phi_{air}\frac{(C_{atm} - 0)}{R}$$

The change in the radius of the unleached zone is described in Equation 8. The thickness of the leached zone is X_0- X.

Equation 8. $$\frac{dX}{dt} = \frac{D\tau_{air}\Phi_{air}C_l}{RC_s}$$

where:

C_l = Concentration of Ca^{2+} ions in the concrete pores (moles/cm^3)
C_s = Bulk concentration of Ca^{2+} ions in the solid concrete (moles/cm^3)
C_{gw} = Concentration of Ca^{2+} ions in the soil pore water (conservatively assumed to be zero (moles/cm^3)
D = Diffusion coefficient of Ca^{2+} ions in concrete (cm^2/s)
X_0 = Initial penetration distance into the concrete (cm)
X = Distance (penetration) in concrete (cm)
N = Molar flux (moles/cm^{2}sec
t = Time (s)
τ_{air} = Tortuosity factor for air
Φ_{air} = Porosity (volume assumed to filled with air)

Chloride induced corrosion was not considered in the INEEL PA because chloride was not present in the groundwater.

4.6.4 References Corrosion of Reinforced Concrete

Alonso, C., C. Andrade, C. Castellote, and P. Castro, "Chloride Threshold values to Depassivate Reinforcing Bars Embedded in a Standardized OPC Mortar," *Cement and Concrete Research*, **30**[7], p.1047-1055, 2000.

Constantinou, A.G. and K.L. Scrivener, 1997. "Microstructural Examination of the Development of Corrosion in Reinforced Concrete," p.134-142, Proceedings of the Materials research Society's Symposium on Mechanisms of Chemical Degradation of Cement-Based Systems, Boston, November 27-30, 1995, Published in Mechanisms of Chemical Degradation of Cement-Based Systems, Eds., K. L. Scrivener and J.F. Young, E&FN SPON, London, 1997.

Garrabrants, A. 2006. Personal Communication with C. Langton, Vanderbilt University, Nashville, TN.

Glasser, F. P., J. Marchand and E. Samson, 2007. "Durability of Concrete – Degradation Phenomena Involving Detrimental Chemical Reactions, Key note address, 2007.

Hansson, C.M., 1984. "Comments on Electrochemical Measurements of the Rate of Corrosion of Steel in Concrete," *Cement and Concrete Research*, **14**[4], p. 574-584.

Hearn, N. and J. Figg, 2001. "Transport Mechanisms and Damage: Current Issues in Permeation Characteristics of Concrete," p. 362-364 Materials Science of Concrete VI, S. Mindess and J. Skalny, Eds., American Ceramic Society, Westerville, OH, 2001.

Hope, B.B, A.K. Ip, and D.G. Manning, 1985. "Corrosion and Electrical Impedance in Concrete," *Cement and Concrete Research*, **15**[3], p. 525-534.

INEEL PA Appendix E, 2003. "Degradation Analysis of the Grouted Tank/vault and Piping System at the Idaho Nuclear Technology and Engineering Center Tank Farm Facility and Preliminary Results for the Detailed Analysis of Releases from the Grouted Pipe and Encasement System, Revision 1,"p. E18, E20, INEEL, Idaho Falls, ID, 2003.

Page, C.L., 1982. "Microstructural Features of Interfaces in Five Cement," *Composites*, p. 140-144.

Page, C.L., N.R. Short, and W.R. Holden, 1986. " The Influence of Different Cements on Chloride-Induced Corrosion of Reinforcing Steel," *Cement and Concrete Research,* **16**[1], p.79-86, 1986.

Samson, E., J. Marchand, 2006, "Multi Ionic Approaches to Model Chloride Binding in Cementitious Materials," 2nd International Symposium on Advances in Concrete Through

Science and Engineering, RILEM Proceedings, PRO, **[51]**, Eds. J. Marchand, et al., RILEM Publications, Quebec City, Canada, 2006.

Samson, E. and J. Marchand, 2007. "Modeling the Effect of Temperature on Ionic Transport in Cementitious Materials," *Cement and Concrete Research*, **37**[3], p.455-468.

Rosenberg, A. and C.M. Hansson, 1989. "Mechanisms of Corrosion of Steel in Concrete," Materials Science of Concrete Volume I, J. Skalny Ed., p. 285-313, American Ceramic Society, Westerville, OH, 1989.

Roy, D.M., 1986. 8th International Congress of Cement Chemistry, p. 362, 1986.

Tuutti, K., "Corrosion of Steel in Concrete," Swedish Cement and Concrete Research Institute, Report No. 4:82, CBI, Stockholm, Sweden, 1982.

US Federal Highway Administration, 1998. "Corrosion Evaluation of Epoxy-Coated, Metallic-Clad, and Solid Metallic Reinforcing Bars in Concrete," Federal Highway Administration, Report No. FHWA-RD-98-153, 1998.

Wheat, H.G., J. Kasthurirangan, and C.J. Kitowski, 1997. "Behavior of Steel in Simulated Concrete Solutions," p.143-150, Proceedings of the Materials research Society's Symposium on Mechanisms of Chemical Degradation of Cement-Based Systems, Boston, November 27-30, 1995, Published in Mechanisms of Chemical Degradation of Cement-Based Systems, Eds., K. L. Scrivener and J.F. Young, E&FN SPON, London, 1997.

5.0 DISCUSSION

5.1 Chemical Degradation of F-Tank Farm Closure Cementitious Barriers

Information obtained from the concrete literature presented in Section 4 was used to assess the potential for the various degradation mechanisms to impact the concrete and grout used to construct and fill the tanks in the FTF. Coupled effects are recognized as important but literature data were insufficient to assess coupled effects.

The analysis presented in this report uses simple empirical relationships and diffusion models because material-specific data are not available. The generalized equations in the INEEL Appendix E analysis were used to calculate penetration depths for this report. Given the limited amount of material-specific information, no uncertainty analysis was performed for this report.

The cementitious barriers identified in the FTF closure concept are either reinforced concrete (tank vault and base mat) or non reinforced grout (annulus and tank fill grouts). A schematic drawing of the FTF cementitious barriers is provided in Figure 5-1. The hydraulic conductivities of the initial state (not degraded) material were obtained from a concrete sample collected from a slab constructed in 1978 that was used as a surrogate for the vault and base mat concrete and a laboratory prepared sample of reducing grout that is in the current specification for closing the FTF tanks. The saturated hydraulic conductivities of the concrete barriers after degradation by the various mechanisms were estimated. In some cases, the saturated hydraulic conductivity was unaffected by the chemical changes. In other cases in which the chemical changes resulted in the formation of expansive phases, the saturated hydraulic conductivity was assumed to increase due to cracking. In this analysis no credit was given to the metal tank or the metal secondary liner.

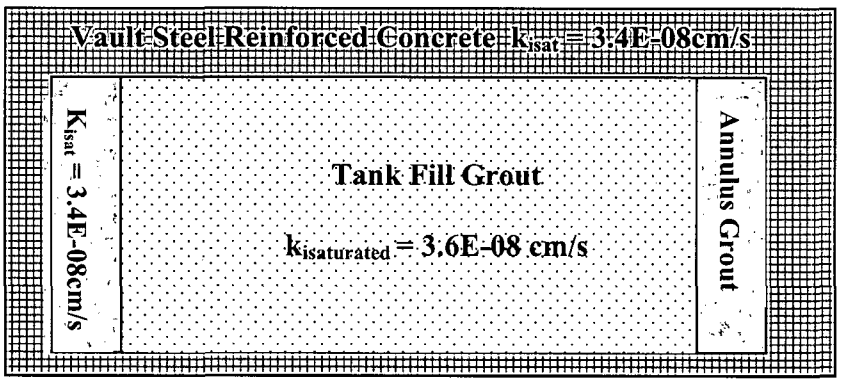

Figure 5-1. Intact SRS F-Tank Farm Cementitious Barriers (not to scale).

This report is limited to a discussion of chemical degradation processes that are known to affect the physical durability which is defined as changes in the microstructure and crack network. Structural degradation (cracking) in response to thermo mechanical forces was not considered in this analysis. However the FTF PA analysis does include fast pathways

[Rosenberger, 2007]. Evolution of the stabilization chemistry (pH and Eh) of the vault concrete and the fill are also discussed elsewhere [Kaplan, 2006 and 2007 (a), (b), (c) respectively]. Assumptions and treatment of macro cracking (fast pathways) and the evolution of the stabilization chemistry are described in detail in the FTF Performance Assessment.

5.2 Sulfate Attack (External)

A linear empirical relationship between the depth of attack and the amount of tricalcium aluminate plus the concentration of Mg^{2+} and SO_4^{2-} in the groundwater was used to calculate the depth of penetration of attack by sulfate and magnesium [INEEL Appendix E, 2006]. The depth of penetration was assumed to be the depth of degradation. See Equation 9 derived from empirical relationships [Atkinson and Hearne, 1984 and Walton, 1990] and used in the INEEL PA [INEEL, 2003]. An explanation of the values used in this calculation is provided in Table 5-1.

The depth of degradation was calculated to be 1.729 E-03 cm/year for the vault concrete which was made with Type I Portland cement (maximum C_3A content in Type I portland cement =12wt%) and 1.153E-03 cm/year for the annulus and tank fill grouts (maximum C_3A content in Type I/II cement = 8 wt%).

Equation 9. $\mathbf{x = 0.55\ C_{C3A}\ (Mg^{2+} + SO_4^{2-})\ t}$

where:
x = depth of concrete degradation (cm)
C_{C3A} = weight percent of tricalcium aluminate in the unhydrated cement
Mg^{2+}, SO_4^{2-} = concentrations of these ions in bulk solution (moles/L)

Penetration rates calculated from Equation 9 and inputs in Table 5-1 did not take into consideration sulfate ion binding by the cement matrix (formation of phases that are not expansive). In addition, the tank fill grout contains fly ash (pozzolan) and slag cement, both of which are routinely used to improve resistance to sulfate attack [ACI 201, 2005]. Consequently, from these two aspect (binding capacity and bulk mineralogy), the calculated rates may be somewhat conservative.

Table 5-1. Values used to calculate rate of sulfate attack and depth of degradation.

Parameter	SRS Vault Concrete	SRS Annulus and Tank Fill Grouts
Inputs		
C_3A (wt %)	12*	8*
Mg^{2+} (moles/L)	0.00021 (5 ppm)**	0.00021 (5 ppm)**
SO_4^{2-} (moles/L)	0.000052 (5ppm)**	0.000052 (5 ppm)**
Output		
Estimated Penetration Rate (cm/year)	1.729E-03	1.153E-03
Estimated Depth of Degradation after 1000 years	1.7 cm	1.2 cm

* The maximum tricalcium aluminate content in Type I cement of 12 wt. % was assumed for the vault concrete. The maximum tricalcium aluminate content in Type I/II cement of 8 wt. % was assumed for the annulus and tank fills [ASTM C-150, 2007].

** Representative ground water concentrations are based on SRS well data. [Strom, 1992, SRS ERDMS, 1997].

5.3 Sulfate Attack (Internal)

Internal sulfate attack of concrete has not been observed at SRS. Consequently, it was not considered in this analysis of degradation of the vault concrete. However, sulfate is present in the residual waste that may be left in the tank. Reactions between the waste and the fill grout have not been studied. Literature data are insufficient to address the likelihood and consequences of this potential mechanism for degradation. Consequently, at this time there is no basis for determining whether reactions if they were to occur would be detrimental to the integrity of the material in the waste-fill zone.

5.4 Alkali-Aggregate Reaction

Alkali-aggregate (silica or carbonate) attack is a coupled diffusion/dissolution/hydration process which occurs when alkalis react with reactive aggregates to produce hygroscopic gel phases. The aggregates used in SRS concrete and planned for use in the tank fill grouts are not highly susceptible to this form of attack. In addition, the concentrations of alkalis in soil pore water and ground water are very low (typical value is less than 1ppm). Consequently this degradation mechanism was not considered for the tank vault concrete and base mat which are in contact with the environment.

Alkalis are present in the residual waste, which may be impossible to completely remove from the tanks. However, because reactions between the washed residual waste and the fill grout have not been studied to date, there is insufficient data to determine what reactions will

occur in this unique chemical environment and to determine the consequences of these reactions with respect to degradation.

The chemical processes responsible for alkali aggregate reaction are similar to if not the same as the beneficial reactions between pozzolans and hydrated cement. The difference is the spatial distribution of the reaction products which are dispersed throughout the matrix in the case of beneficial pozzolans versus concentrated at matrix aggregate interfaces in the case of alkali aggregate degradation. Literature data are insufficient to address the likelihood and consequences of this potential mechanism for degradation. Consequently this degradation mechanism was not considered for the tank fill material due to lack of data on the waste-fill reactions and physical consequences of these reactions.

5.5 Acid Attack

The depth of penetration from acid attack on the vault concrete and fill was represented by ionic diffusion of calcium ions through aqueous pore water. Diffusion is driven by the concentration gradient between ions in the cementitious material versus ions in the environmental water.

In the penetration rate equation (Equation 10), the concentration of Ca^{2+} in the groundwater (soil pore water) was assumed to be zero, which maximizes the concentration gradient and consequently the penetration rate. The values used for the concentrations of Ca^{2+} in the cementitious pore water and in the cementitious solids were the same as those used in the INEEL PA Appendix E and are reasonable for cement paste pore solution and the bulk composition of concrete with inert aggregates such as the quartz sand and granite and schist aggregates used for the SRS tank closures.

The INEEL equation were combined with SRNL diffusion data as presented in Phifer et al., 2006, to generate equations 11 through 13. Results are provided in Table 5-2.

Equation 10. $$X = \left(2 D_m \tau \Phi \frac{(C_l - C_{gw})t}{C_s} \right)^{1/2}$$ [INEEL PA Appendix E, 2003]

Equation 11. $$X = \left(2 \frac{D_m \Phi}{\tau'} \frac{(C_l - C_{gw})t}{C_s} \right)^{1/2}$$ SRNL diffusion nomenclature [Phifer, et al., 2006]

Equation 12. $$D_e = \frac{D_m}{\tau'}$$ SRNL diffusion nomenclature [Phifer, et al., 2006]

Equation 13. $$X = \left(2D_e \Phi \frac{(C_l - C_{gw})t}{C_s} \right)^{1/2}$$

where:

X = Depth of penetration
D_m = Molecular diffusion coefficient for Ca^{2+} ions
D_e = Effective diffusion coefficient for Ca^{2+} ions, ($D_e = D_m / \tau'$)
τ = Tortuosity factor (≤ 1)
τ' = SRNL Tortuosity factor ($1/\tau \geq 1$)
Φ = Porosity (volumetric water content)
C_l = Calcium ion concentration in pores
C_{gw} = Calcium ion concentration in groundwater
C_s = Calcium ion concentration attributed to $Ca(OH)_2$ in bulk concrete
t = Time

Table 5-2 Values used to calculate rate of acid attack.

Parameter	SRS Vault Concrete	SRS Annulus and Tank Fill Grouts
Inputs		
D_e[(a)] (cm^2/sec)	8E-07	8E-07
τ[(a)]	Value included in D_e	Value included in D_e
Φ[(b)] Water exchangeable porosity	0.168	0.266
C_l[(c)] (mol/cm^3)	2.70E-06	2.70E-06
C_{gw}[(d)] (mol/cm^3)	0	0
C_s[(e)] (mol/cm^3)	5.4E-04	5.4E-04
Output		
Estimated Penetration Depth at 1000 years	6.5cm Rate is time dependent. This assumes that 100 % of the calcium hydroxide in the penetrated zone is leached.	8.2 cm Rate is time dependent. This assumes that 100 % of the calcium hydroxide in the penetrated zone is leached.

(a) The effective diffusivity, D_e, is documented elsewhere [Dixon and M. Phifer, 2007]. $D_e = D \div$ tortuosity, where $D = D_{molecular}$. Consequently, a separate tortuosity term was not included in the calculation. Diffusion coefficient definitions and terminology are presented elsewhere [Phifer, et al.., 2006].
(The value for De is close to the value used for D/Φ in the Idaho PA.)

(b) Porosity values vault and base mat concrete and for reducing grout were obtained from WSRC-STI-2007-00369 [Dixon, 2007].

(c) Pore solution data from Idaho PA

(d) Assigned value of 0 which results in the greatest concentration gradient and is the most conservative case.

(e) Estimated value assumed that concrete contains 27.5 kmol/m3 CaO and the 3000 psi concrete is only 13 % cement and of the cement, only 15% is hydrated to $Ca(OH)_2$. The penetration value assumes it is all leachable.

The calculation contains the assumption that the acid component diffuses into the concrete via the aqueous phase and that the dissolution rate of solid phases is instantaneous. An improvement to the current model would include the solubilities of all calcium phases in the cementitious material plus new phases formed as the result of acid leaching.

5.6 Carbonation

In the carbonation process, carbon dioxide from the atmosphere reacts with calcium hydroxide in the cement material to form calcium carbonate. This process is only a degradation mechanism for reinforced concrete. Pore water in equilibrium with calcium hydroxide has a high pH (12.5) which stabilizes the oxide layer surrounding the steel and prevents active corrosion. On the other hand, pure water in equilibrium with calcium carbonate has a pH of 8.4 and fails to stabilize the oxide layer and allows active corrosion.

For non-reinforced cementitious material, carbonation has been reported to seal pores and create a protective layer (rind) on exposed surfaces. Consequently, carbonation was only considered as a degradation mechanism for the steel reinforced cementitious materials, i.e., base mat and concrete vault.

5.7 Carbonate-Induced Rebar Corrosion

The corrosion products formed when rebar oxidizes (corrodes) have a higher volume than the original metal. The resulting expansion can crack the surrounding concrete. In this analysis the depth of penetration of CO_2 represents the depth of degradation caused by rebar corrosion.

The depth of penetration of CO_2 into reinforced concrete is a gaseous diffusion controlled process. In Equation 10, the external source of the CO_2 is the atmosphere (0.03 volume %). (The small amount of CO_2 dissolved in water in equilibrium with the atmosphere was ignored). This assumption maximizes the concentration gradient which in turn maximizes the depth of penetration.

Input values for Equation 10 were obtained from several sources. The binary diffusion coefficient for CO_2 in air was 9.60E-04 m^2/min (505 m^2/y) [Lide, 1995].[29] The bulk concentration of calcium hydroxide in hardened concrete was estimated to be 5.4E-01 kmol/m^3. The estimated value assumes that concrete contains 27.5 kmol/m3 CaO and the 3000 psi concrete is only 13 % cement and of the cement, only 15% is hydrated to Ca(OH)2. The penetration value assumes it is all leachable.[30]

Tortuosity factors of 9.2E-03 and 1.7E-02 were used for concrete and fill, respectively. These values are calculated from the Millington-Quirk model, Equation 11 [Jin, 1996]. The

[29] This value is different than the value stated in the INEEL PA of 1.55 E-04 m^2/y.

[30] This value is lower than that assumed in the Idaho PA and results in a greater depth of penetration, all other values being equal. Neither of these assumptions takes into account the complex reaction fronts observed in actual carbonated material.

difference in the tortuosity factor for the vault concrete and fill material is due to the difference in the porosities measured for surrogate tank vault concrete and reducing grout fill, 16.8 and 26.6 volume percent, respectively.

Equation 14. $\tau = a^{10/3} / \Phi^2$

where:

a = volumetric air content assuming 50 % saturation (This allows for gas phase transport in the cementitious material.)

Φ= cementitious barrier porosity

Equation 15 $$X = \left(2D_{air} \tau \Phi_{air} \frac{(C_{atm})t}{C_s} \right)^{1/2}$$

where:

X = Depth of penetration
D_{air} = Binary diffusion coefficient for air/CO_2
τ = Tortuosity factor of gas in the concrete
Φ_{air} = Volumetric air content in concrete assuming 50 % saturation
C_{atm} = Concentration of total inorganic carbon in air (present as CO_2)
C_s = Bulk Concentration of $Ca(OH)_2$ in concrete t = time

Table 5-3 Values used to calculate rate of carbonation.

Parameter	SRS Vault Concrete	SRS Annulus and Tank Fill Grouts
Inputs		
D_{air} [a] (m^2/yr)	5.05E+02	5.05E+02
τ [b, c]	9.2E-03	1.7E-02
Φ_{air} [c]	0.084	0.133
C_{atm} [d] ($moles/cm^3$)	3.00E-05	3.00E-05
C_s [e] ($moles/cm^3$)	5.4E-01	5.4E-01
Output		
Estimated Penetration Depth at 1000 years	20.8 cm Rate is time dependent This assumes that 100 % of the calcium hydroxide in the penetration zone is carbonated	35.6 cm Rate is time dependent. This assumes that 100 % of the calcium hydroxide in the penetration zone is carbonated

[a] CRC, 1995. The value used in this calculation is different than the value reported in the INEEL PA Appendix E which was 1.55E-04 m^2/y but using the CRC value produces similar results as those presented in the Appendix E Figure E-4.
[b] Millington-Quirk Formula used to calculate tortuosity factor = $a^{10/3}/\Phi^2$ where "a" equals the volumetric air content [Jin, 1996].
[c] WSRC-STI-2007-00369 for air volume plus the assumption of 50 % saturation from INEEL Appendix E
[d] INEEL used density of air 1.2 kg/m^3.
[e] Assumed that 10 % of the calcium in concrete is $CaOH_2$ which is approximately 0.15g/cc of cementitious material.

5.8 Chloride-Induced Rebar Corrosion

Chloride-induced rebar corrosion was not considered in this analysis because the concentration of chloride ions in SRS ground water and soil pore water is very low. Typical ground water for SRS well samples are about 2 ppm [Strom, 1992]. Chloride in the cement used to construct the tank vaults is of interest but data are not available. Samples of 29 year old 3000 psi concrete were collected, tested and used as surrogates for the vault and base mat concrete. This material was not analyzed for chloride. However, inspection of the rebar in this concrete showed no sign of corrosion.

5.9 References Degradation Calculations

ACI 201-2005. "Guide to Durable Concrete," American Concrete Institute, Farmington, MI 48333.

ASTM C-150, 2007. "Standard Specification for Portland Cement," American Society for Testing and Materials, Conshohocken, PA.

Atkinson, A, and H. A. Hearne, 1984. "An Assessment of the Long-Term Durability of Concrete in Radioactive Waste Repositories," AERE-R11456, Harwell, U.K., 1984.

Dixon, K.L. and M.A. Phifer, 2007. "Hydraulic and Physical Properties of Tank Grouts for FTF Closure," STI-2007-00369, October, 2007, Washington Savannah River Company, Aiken SC 29808.

ERDMS, 2007. Environmental Restoration Data Management System, J. Wurster data base manager, Washington Savannah River Company, Aiken SC 29808.

INEEL PA Appendix E, 2003 Revision 1. "Degradation Analysis of the Grouted Tank/vault and Piping System at the Idaho Nuclear Technology and Engineering Center Tank Farm Facility and Preliminary Results for the Detailed Analysis of Releases from the Grouted Pipe and Encasement System," INEEL, Idaho Falls, ID, 2003.

Jin, Y. and W.A. Jury, 1996. "Characterizing the Dependence of Gas Diffusion Coefficient on Soil Properties," Soil Science Society of America Journal, **60**[1]. p. 66-71.

Lide, D.R., 1995. Handbook of Chemistry and Physics, CRC Press, 1995.

Phifer, M.A., M.R.Millings, and G.P.Flach, 2006. "Hydraulic Property Data Package for the E-area and Z-Area Soils, Cementitious Materials, and Waste Zones," p.176-192, WSRC-TR-2006-00198, Washington Savannah River Company, Aiken SC 29808.

Rosenberger, K.H., 2007. Personal communication with C.A. Langton.

Strom, R.N. and D.S. Kaback, 1992. "SRP Baseline Hydrogeologic Investigation: Aquifer Characterization, Groundwater Geochemistry of the Savannah River Site and Vicinity (U)," WSRC-RP-92-450, p. 72-83, Westinghouse Savannah River Company, Aiken SC 29808.

Subramanian, K.H., 2007. "Life Estimation of High Level Waste Tank Steel for F-tank Farm Closure Performance Assessment," WSRC-STI-2007-00061, Rev. 1. October 1-2007, Washington Savannah River Company, Aiken SC 29808.

Walton, J.C., L.E. Plansky and R.W. Smith, 1990. "Models for Estimation of Service Life of Concrete Barriers in Low-Level Radioactive Waste Disposal," NUREG/CR—5542, TI91 000576, EG&G Idaho, Inc., Idaho Falls, ID 83415.

Table 5-4. Summary of Chemical Attack Mechanisms Relevant to Tank Concrete and Fill.

Attack	Process	Control	Comments	Expression and Effect on Permeability
Acid Attack (Leaching)	Coupled dissolution/ diffusion/leaching	Acid concentration Ionic Diffusion through water	Source of acid is infiltrating rain water. Potential acids are from atmospheric gas (CO_2, NOx, SOx) or Organic acids from overlying soil	Vault Concrete (Reinforced). Increase in permeability, porosity and strength loss. Fill. Increased porosity and change in stabilization chemistry/mineralogy of the system from high pH of 13 to 8.5 Progression of reaction front inward from surfaces and fracture surfaces. Rate depends on acid concentration
Carbonation	Coupled diffusion / dissolution / precipitation process	Carbonate or CO_2 Ionic Diffusion through water for 100 % Saturated Condition Gas Diffusion for Unsaturated Grout	Air is the source of CO_2. Residual waste is a source of carbonate.	Vault Concrete: Increase in permeability and strength loss. Fill: No or only slight change +/- in permeability due to $CaCO_3$ precipitation in pores and on surfaces Progression of reaction front inward from surfaces and fracture surfaces. Rate depends gas or aqueous diffusion Gas phase transport is ~1000X faster than diffusion through water.
Sulfate Attack	Coupled diffusion / dissolution / precipitation process	Sulfate (Internal and External) Ionic Diffusion through water	Soil does not contain sulfate Residual waste is a source of sulfate	Vault Concrete. NA Negligible soluble sulfate in soil Fill: Calcium aluminosulfate-carbonate phases may form at the waste zone-fill contact at the bottom of the closed tanks. Data is required to evaluate consequences.
Alkali Aggregate Reaction	Coupled diffusion / dissolution / hydration process	Na^+, reactive aggregate, water	Aggregates have low reactivity	Vault Concrete. NA Negligible source of alkali in soil Fill: Potential reactions at the waste zone-fill contact at the bottom of the closed tanks. Data is required to evaluate consequences.
Reinforcing Steel Corrosion	Coupled diffusion / dissolution / precipitation process	Carbonation Corrodents (Cl^-) Oxygen, Water Ionic Diffusion through water (CO_2 can also diffuse through air)	Soil does not contain soluble corrodents eg. Cl^-	Vault Concrete. Cracking due to expansion which results in strength loss and increased hydraulic conductivity. Loss of passivation by carbonation, expansive from iron hydration products Fill: Not Applicable

6.0 CONCLUSIONS

The SRS disposal environment is very benign with respect to chemical degradation of the reinforced concrete vaults and the tank fill grout material. Consequently, the degradation due to chemical processes will progress at a very slow rate.

Carbonation was identified as the most aggressive chemical degradation mechanism. The thickness of the carbonated zone after 1000 years was calculated to be 20.8 cm for material with the properties of the surrogate vault concrete. For material with the properties of the tank fill reducing grout, the carbonation depth was calculated to be 35.6 cm after 1000 years of direct contact with atmospheric air in the soil pores.

Depths of penetration for several chemical species known to cause degradation were calculated for two types of material:[31]

1. Surrogate Vault Concrete. Twenty nine year old 3000 psi concrete cored from a slab on grade in P-Area.
2. Representative Tank Fill Grout. Reducing Grout prepared according to the mix in SRS Specification C-SRP-F-00047 Rev. 2.

Chemical reactions responsible for concrete degradation were identified, and methodologies for predicting rates of degradation were reviewed. The chemical degradation mechanisms evalutated were: sulfate attack (internal and external), acid leaching (decalcification), carbonation, alkali aggregate attack, and cracking from rebar corrosion (carbonate-induced and chloride-induced corrosion).

For this evaluation, the depths of penetration of the chemical corrodents were assumed to be equivalent to the depth of degradation. Diffusion transport of the corrodent species through the pores in the cementitious material was assumed. Equations for single species diffusion were used. This is a very simplistic approach. A more sophisticated approach requires additional material characterization data and advanced multi ionic transport codes specifically designed for concrete service life predictions.[32]

Penetration distances for the acid attack and carbonation, cracking due to rebar corrosion were calculated using equations for ionic (Ca^{2+} ions) and gaseous (CO_2) diffusion models. Concentration gradient is the driving force for transport in these models. Porosity is also an important parameter.

---

[31] Different porosities were used in the rate calculations. Concentrations of $Ca(OH)_2$ were assumed to be those in the concrete. No adjustments were made for the effects of pozzolans in either the concrete or fill grout.

[32] Advanced service life prediction models for concrete structures were not used for this analysis. These models require concrete-specific properties, such as, moisture, ionic, and gas diffusion coefficients, pore solution chemistry, porosity, pore size distribution, degree of saturation, cement chemistry and mineralogy, and thickness of rebar cover. They also required environment-specific characterization data.

An example of software for service life prediction is the STADIUM code which is being developed by SIMCO Technologies, Inc.

An empirically derived equation was used for sulfate attack. This form of deterioration involves a complex series of diffusion/dissolution/ precipitation processes, and the overall consequences (loss of sound material) were obtained from experimental testing. Alkali aggregate attack was also evaluated.

Each degradation mechanism was evaluated independent of the others. Coupled effects and the potential for non deleterious binding of the chemical species within the cement matrix phases were not considered. Results are presented in Table 6-1. Each material was assumed to be in direct contact with the environment supplying the corrosive chemicals. In this model, the annulus grout will not begin carbonating until the vault concrete is degraded, because the geometry of the engineered barriers is one of contacting concentric cylinders. (The roof and base mat thicknesses must also be taken into account as well as the actual configuration which includes metal liners and tanks.)

The effect of chemical degradation on permeability of each of the three cementitious barriers in the FTF Closure concept depends on how the attack is expressed. The chemical degradation mechanisms and consequences of these processes are summarized as follows:

- The saturated permeability of the initial vault concrete was estimated to be 3.4E-08 cm/s. This value was obtained from measurements on 29 year old 3000 psi reinforced concrete which was used as a surrogate. Carbonation will result in loss of passivation and subsequent corrosion of rebar. The rebar corrosion products are expansive and will cause cracking. The time of cracking will be offset from the time the carbonation front reaches the rebar because sufficient corrosion products must be formed to exert force on the concrete. In this analysis, depth of carbonation is a time dependent function. In 1000 years it is estimated to penetrate the vault concrete 21 cm.
  - The permeability for cracked concrete resulting from rebar corrosion due to carbonation was estimated to be 100 times higher than the initial permeability [Flach, 2007].

- The saturated permeability of the annulus concrete was estimated to be 3.6E-08 cm/s based on measurements of samples of the reducing grout prepared in the laboratory. The overall effect of carbonation will be precipitation of calcite, $CaCO_3$ which seals surfaces and plugs pores. Consequently, with no potential for rebar corrosion, carbonation will have no or very little effect on the annulus grout.
  - The permeability will remain at about 3.6E-08 cm/s. The same holds for tank fill grout for tanks with no cooling coils.

- Tanks that contain cooling coils will experience carbonation after the tank has corroded or after fast path ways develop. The rate of carbonation will be slightly faster than that estimated for the vault concrete because the porosity of the grout is slightly higher. The depth of penetration after 1000 years exposure to the atmosphere was 36 cm.

This evaluation was limited to chemical degradation mechanisms which are known to affect the microstructure, mechanical and engineering properties of materials containing portland cement. It does not address degradation caused by mechanical forces or evolution of the stabilization chemistry (pH and Eh) of the material.

Table 6-1. Summary of Depth of Penetration (Thickness of Affected Material) for SRS Tank Closure Cementitious Barriers.

Mechanism	Penetration Depth at 1,000 years (cm)	
	Vault Concrete Material	**Tank Fill Grout Material**
Sulfate Attack (Exernal)	1.7	1.2
Sulfate Attack (Internal)	Not Applicable Basis: Lack of this type of degradation in SRS concrete since early 1950s.	Not Estimated Basis: Sulfates are present in the residual tank waste but data on tank waste-grout chemistry and physical consequences are not available.
Alkali Aggregate Attack	Not Applicable Basis: Low alkali content (~5mg/L) of soil and groundwater and use of resistant aggregate is SRS concretes and grouts.	Not Estimated Basis: Alkalis are present in the residual tank waste but data on tank waste-grout chemistry and physical consequences are not available.
Acid Attack (Calcium Leaching)	6.5 Basis: Diffusion controlled by concentration gradient. Ca^{2+} in ground water assumed to be 0 mg/L which is less than typical values of 5 mg/L. Ca leaching was assumed to preferentially dissolve $Ca(OH)_2$. $Ca(OH)_2$ in the vault concrete was estimated at 5.4E-04 mol/cm^3. Porosity of vault concrete is 16.8 vol. percent	8.2 Basis: Same but porosity of Reducing Grout was 26.6 vol. %
Carbonation	20.8 Basis: Diffusion controlled by concentration gradient. Atmosphere is the source of CO_2 (0.03 vol. % CO_2). One mole of C fromCO_2 reacts with 1 mole of $Ca(OH)_2$ to form $CaCO_3$ $Ca(OH)_2$ in the vault concrete was estimated at 5.4E-01$kmol/m^3$. Porosity of vault concrete is 16.8 vol. percent.	35.6 Basis: Same but porosity of Reducing Grout was 26.6 vol. %
Concrete Cracking due to Rebar Corrosion		
Carbonate-Induced Corrosion	20.8 Basis: The depth of penetration of the carbonation front can be used as a conservative estimate for depth of deterioration (cracking) due to rebar corrosion since carbonation lowers the alkalinity of the pore solution and reduces the stability of the corrosion resistant oxide film on the steel.	Not Estimated Basis: The annulus and tank fill grouts do not contain rebar. Depth of penetration of carbonate does not correlate with active corrosion of steel. Additional chemical conditions are required for steel corrosion. These conditions are discussed elsewhere [Subramanian, 2007]. Rates and consequences of corrosion of the steel tanks, secondary containment liners and cooling coils were not evaluated.
Chloride-Induced Corrosion	Not Estimated Basis: The chloride concentration in the groundwater and soil pore water is very low (~1 mg/L). The chloride binding capacity and the initial chloride content in the concrete have not been determined.	Not Estimated Basis: Same as for carbonate-induced corrosion and for chloride induced-corrosion of the vault concrete.

7.0 RECOMMENDATIONS

As a result of this exercise, several areas for further study were identified and are listed below:

- Service Life predictions for the surrogate vault concrete and representative tank fill grout should be determined using multi ionic models such as STADIUM®, developed by SIMCO Technologies, Inc. Predictions will be limited to common service lives of concrete structures of 50 to 100 years but this is useful information for extrapolation to longer times required for performance assessment of low level waste disposal facilities.

- Diffusion data, solubility data and pore solution chemistry data are required for the advanced multi ionic transport models used to predict service life. These data should be obtained for surrogate and representative materials.

- Prediction of the pore solution chemistry over long times and the effect of this chemical environment on rebar and tank steel corrosion should be investigated.

- The unsaturated soil-cementitious barrier interface should be characterized with respect to:
  - Development of chemical and microstructural zones in both media and
  - Moisture and gas transport across the interface.

  Laboratory testing and instrumented test beds are recommended to obtain the relevant parameters and relationships.

- The degree of saturation of the cementitious barriers in the disposal environment should be determined as a function of time and degradation scenarios. This information should be factored into transport processes.

- Fracture transport should be evaluated with respect to chemical degradation processes and also the chemical environment required for stabilization.

- Residual waste-cementitious material interactions should be investigated with respect to formation of new phases, potential for expansive reactions and consequences of these reactions, and leachability of the contaminants. The physical properties of the waste-cement material zone should be characterized.

- Permeabilities of samples of concrete and tank fill grout degraded by carbonation and the other chemical mechanisms described in this report should be measured. The current surrogate material is a sandy clay soil and the permeability of this soil is assumed to approximate the permeability of degraded concrete.
  - Consider computer simulations for the evolution of the microstructure and macrostructure of the concrete in response to the various forms of degradation.

Distribution:

S. E. Aleman, 773-42A
H. H. Burns, 999-W
T. W. Coffield, 766-H
R. D. Deshpande, 766-H
K. L. Dixon, 773-42A
R. E. Edwards, 773-A
G. P. Flach, 773-42A
J. C. Griffin, 773-A
J. R. Harbour, 999W
M. H. Layton, 766-H
J. E. Marra, 773-A
J. L. Newman, 766-H
D. K. Peeler, 999W
M. A. Phifer, 773-42A
T. C. Robinson, 766-H
L. B. Romanowski, 766-H
K. H. Rosenberger, 766-H
R. R. Seitz, 773-43A
E. L. Wilhite, 773-43A